

Autophagy inhibition as a potential future targeted therapy for ETV6-RUNX1-driven B-cell precursor acute lymphoblastic leukemia

Roel Polak,¹ Marc B. Bierings,^{2,3} Cindy S. van der Leije,⁴ Mathijs A. Sanders,⁴ Onno Roovers,⁴ João R. M. Marchante,¹ Judith M. Boer,¹ Jan J. Cornelissen,⁴ Rob Pieters,³ Monique L. den Boer^{1,3*} and Miranda Buitenhuis^{4*}

¹Department of Pediatric Oncology, Erasmus MC - Sophia Children's Hospital, Rotterdam; ²Department of Pediatric Oncology, University Medical Center Utrecht; ³Princess Máxima Center for Pediatric Oncology, Utrecht and ⁴Department of Hematology, Erasmus Medical Center, Rotterdam, the Netherlands

*MdB and MB contributed equally to this work.

©2019 Ferrata Storti Foundation. This is an open-access paper. doi:10.3324/haematol.2018.193631

Received: March 18, 2018.

Accepted: October 30, 2018.

Pre-published: October 31, 2018.

Correspondence: *MONIQUE L. DEN BOER*

m.l.denboer@prinsesmaximacentrum.nl

SUPPLEMENTARY DATA

Autophagy inhibition as a potential future targeted therapy for ETV6-RUNX1 driven B-cell precursor acute lymphoblastic leukemia

Authors: Roel Polak, Marc B. Bierings, Cindy S. van der Leije, Mathijs A. Sanders, Onno Roovers, Joao R. M. Marchante, Judith M. Boer, Jan J. Cornelissen, Rob Pieters, Monique L. den Boer & Miranda Buitenhuis

SUPPLEMENTARY METHODS

Cell lines

B-cell precursor acute lymphoblastic leukemia (BCP-ALL) cell lines NALM6 (B-Other; IGH-DUX4), REH (ETV6-RUNX1), and 697 (TCF3-PBX1), T-ALL cell lines JURKAT (hypotetraploid) and LOUCY (del(5); t(16;20)) and human embryonic kidney cell line HEK293T were obtained from DSMZ (Braunschweig, Germany) and used only at low passages. REHS1 (REH subclone #1; ETV6-RUNX1) is a ETV6-RUNX1 positive cell line with identical genetic background as REH, but with different phenotypic characteristics (proliferation and drug resistance profiles). DNA fingerprinting was performed routinely on these cell lines to verify their genetic status. ALL cell lines were cultured in RPMI-1640 medium (Gibco, Life Technologies, Bleiswijk, the Netherlands) supplemented with 10% fetal calf serum (FCS) and 1% penicillin-streptomycin at 37 °C and 5% CO₂. HEK293T cells were cultured in high glucose Dulbecco's Modified Eagle's Medium with Glutamax (Gibco) supplemented with 10% FCS and 1% penicillin-streptomycin at 37 °C and 5% CO₂.

Isolation of CD34-positive hematopoietic cells from cord blood

Mononuclear cells were isolated from umbilical cord blood (UCB) using Lymphoprep sucrose-gradient centrifugation (1.077 g/ml, Nycomed Pharma, Oslo, Norway). Immunomagnetic cell separation, using magnetic beads coated with CD34 antibodies (Miltenyi Biotec, Gladbach, Germany), was performed to isolate CD34-positive hematopoietic progenitor cells (CB-CD34⁺ cells). Cells were cultured in Iscove's Modified Dulbecco's Medium (Gibco) supplemented with 10% FCS, 50µM β-mercaptoethanol, 1% penicillin-streptomycin, 2mM glutamine, stem cell factor (SCF; 50ng/mL; Peprotech) and fms-like tyrosine kinase-3 ligand (Flt3L; 50 ng/mL; Peprotech) at 37°C and 5% CO₂. UCB was obtained after informed consent was provided according to the Declaration of Helsinki.

Protocols were approved by the ethics committee of the Erasmus University Medical Centre in Rotterdam.

Isolation of primary BCP-ALL leukemic blasts from patients

Bone marrow aspirates were obtained from children with newly diagnosed BCP-ALL prior to treatment. Immunophenotype and genetic subtype were determined by local hospital procedures and monitored by the central diagnostic laboratory of the Dutch Childhood Oncology Group (DCOG) in The Hague. Primary BCP-ALL cells were subsequently isolated as previously described (1). We included 654 ALL patients including 172 ETV6-RUNX1 positive BCP-ALL patients and 401 ETV6-RUNX1 negative BCP-ALL patients. In short, mononuclear cells were collected using Lymphoprep sucrose-gradient centrifugation (1.077 g/ml, Nycomed Pharma, Oslo, Norway). To determine the percentage of leukemic cells in the mononuclear cell fraction, May-Grünwald-Giemsa staining was performed on cytospin preparations. If necessary, the samples were further enriched, to obtain at least 95% leukemic blasts, by depletion of normal hematopoietic cells using anti-CD lineage marker coated magnetic beads (Dynal, Oslo, Norway). Cells were cultured in RPMI Dutch-modified medium (Gibco) supplemented with 20% FCS, Insulin transferrin sodium selenite (ITS), glutamin and gentamycin at 37 °C and 5% CO₂. Bone marrow aspirates were obtained after informed consent was provided according to the Declaration of Helsinki. Protocols were approved by the ethics committee of the Erasmus University Medical Centre in Rotterdam.

Isolation and characterization of primary MSCs

Mesenchymal stromal cells (MSCs) were isolated, as previously described (2), from bone marrow aspirates collected during diagnostic procedures. In short, colony-forming MSCs were selected by culturing bone marrow aspirates in low glucose DMEM (Gibco)

supplemented with 15% FCS, 1% penicillin-streptomycin, vitamin C, and fibroblast growth factor (FGF) at 37°C and 5% CO₂. A panel of positive (CD44/ CD90/ CD105/ CD54/ CD73/ CD146/ CD166/ STRO-1) and negative surface markers (CD19/ CD45/ CD34) was used to characterize primary MSCs. Flow cytometric analysis was performed using the human mesenchymal stem cell marker antibody panel (R&D Systems, Minneapolis, MN, USA) and the monoclonal antibodies CD54-PE, CD73-PE, CD34-PE, and IgG1-PE (BD Biosciences, San Jose, CA, USA). The multilineage potential of the selected MSCs was confirmed by allowing the cells to differentiate towards adipocytes (Oil Red O staining), osteocytes (*Alizarin Red S* staining), and chondrocytes (Col2a/Thionine/Alcian Blue staining).

Production of bicistronic retrovirus and retroviral transduction of CB-CD34⁺ cells

To generate retrovirus, bicistronic retroviral DNA constructs were used expressing the *ETV6-RUNX1* fusion gene and enhanced Green Fluorescent Protein (eGFP). As a control, a construct expressing only eGFP was used. Both vectors consisted of a pMSCV promoter region, an internal ribosomal entry site and an ampicillin resistance cassette. HEK293T cells were co-transfected with these constructs and second-generation retroviral packaging vectors using XtremeGENE 9 transfection reagents (Roche, Basel, Switzerland). Viral particles were collected in IMDM 48 hours after transfection. CD34⁺ hematopoietic progenitors were pre-cultured overnight as described above, upon which cells were divided in two fractions. One fraction was transduced with ETV6-RUNX1-IRES-eGFP, while the other fraction was transduced with control EV-IRES-eGFP. Transductions were performed with fresh retrovirus in retronectin (Takara, Otsu, Japan) coated wells.

Fluorescence activated cell sorting of transduced CB-CD34⁺ cells

Transduced CB-CD34⁺ cells were sorted using a BD ARIA II sorter (BD Biosciences) after

staining with DAPI (Sigma) and PeCy7-conjugated CD34 antibody (BD Biosciences). The DAPI negative, CD34 positive and GFP positive population (see Fig. S8C for gating strategy) was used for further experiments. The purity of the sorts, as determined by flowcytometric analysis of the sorted cells, was in all cases at least 95% (see Fig. S4B for a representative post-sort analysis of purity).

Linear RNA amplification and gene expression profiling of CB-CD34⁺ cells

After sorting, DAPI⁻ CD34⁺ GFP⁺ CB-CD34⁺ cells were lysed and RNA was extracted using Nucleospin RNA XS extraction columns according to manufacturer's protocol (Macherey-Nagel, Düren, Germany). Quality of RNA was determined by on-chip-electrophoresis using a RNA Pico Chip according to manufacturer's protocol (Agilent Technologies, Santa Clara, CA, USA). RNA Integrity scores (RIN) were higher than 8 for all samples. RNA was subsequently linearly amplified using the Nugen WT-Amplification™ pico system (Nugen, San Carlos, CA, USA). This system is based on RNA-dependent DNA polymerase activity and was previously reported to be most suitable for amplification and gene expression of picograms of input RNA (3). Samples were run on Affymetrix GeneChip Human Genome U133 Plus 2.0 microarrays (Santa Clara, CA, USA). Data were normalized using vsnRMA and analyzed using a linear mixed model (4). The model was fitted to ETV6-RUNX1, RUNX1-RUNX1T1 and EV data derived for each respective umbilical cord blood donor. Data derived from the RUNX1-RUNX1T1 transduced umbilical cord blood donors were omitted for further analyses in this manuscript and singularly used for estimating the within umbilical cord blood variance. Genes were considered differentially expressed when $p \leq 0.05$ after multiple testing correction using false discovery rate (FDR). Differential gene expression was visualized using TIBCO Spotfire software (Perkin Elmer, Waltham, MA, USA).

Microarray data are available in the ArrayExpress database

(<http://www.ebi.ac.uk/arrayexpress>) under accession number E-MTAB-3466.

Gene expression profiling of primary BCP-ALL leukemic blasts from patients

Sample preparation and gene expression profiling of leukemic blasts derived from bone marrow aspirates was performed as earlier described (5). In short, DNA and total RNA were isolated using TRIzol reagents (Invitrogen Life Technologies, Breda, the Netherlands) or using the QIAamp DNA Blood mini kit (Qiagen, Venlo, the Netherlands) in accordance with the manufacturer's protocol and subsequently RNA quality was determined using a Bioanalyzer 2100 (Agilent, Amstelveen, the Netherlands). Only samples with an RNA integrity value >7 were processed further. cDNA and cRNA were synthesized using an in vitro transcription one-cycle kit (Affymetrix, Santa Clara, CA). Affymetrix U133 plus 2.0 gene-expression microarrays were processed, and data were extracted, as described previously (1). Microarray data are available in the Gene Expression Omnibus database (<http://www.ncbi.nlm.nih.gov/geo/>).

Ingenuity Pathway Analysis

Gene networks were generated and functional analysis of differential gene expression was performed using QIAGEN's Ingenuity Pathway Analysis (IPA, QIAGEN, Redwood City, USA). The expected increase or decrease of biological functions, based on the observed change in gene expression, was defined as a regulation Z score and was considered significant when larger than 2 or smaller than -2. P-values represent results of a right-tailed Fisher's Exact Test after Benjamini-Hochberg multiple testing correction.

Western blot

For protein analysis, cells were lysed using a cold lysis buffer containing 25 mM Tris pH 7.4, 150 mM NaCl, 5mM EDTA pH 8.0, 1% Triton X-100, 10% Glycerol, 10 mM Sodium-pyrophosphate, 1 mM Sodium-orthovanadate, 10 mM Glycerolphosphate, Dithiothreitol, Phenylmethylsulfonyl Fluoride, Aprotinin and Sodium-Fluoride. Equal amounts of protein were separated on a 10% acrylamide gel and subsequently blotted on a nitrocellulose membrane using the Trans-Blot Turbo Transfer System (Bio-rad, Hercules, CA, USA). Primary antibodies used were: β -actin (ab6276, Abcam, Cambridge, UK), LC3B (#2775, Cell Signaling, Danvers, MA, USA), SQSTM1/p62 (#8025, Cell Signaling), Vps34 (#3358, Cell Signaling) and Vps34 (#4263, Cell Signaling). Fluorescently labeled secondary IRDye antibodies were purchased from LI-COR Biosciences (Lincoln, NE, USA) and blots were scanned using an Odyssey Infrared Imaging System (LI-COR Biosciences).

Reverse Phase Protein Array

Reverse phase protein arrays were performed in collaboration with prof. dr. E. Petricoin (George Mason University, Manassas, VA, USA) as previously described (6). In short, normal bone-marrow samples and pediatric BCP-ALL patient cells were lysed in Tissue Protein extraction reagent (T-PER; Pierce, Thermo Scientific, Waltham, MA, USA), containing 300mM NaCl, 1 mM orthovanadate and protease inhibitors. Lysates were spotted twice in triplicate on glass-backed nitrocellulose-coated array slides. Reverse-phase protein arrays were performed according to manufacturer's protocol. Data were normalized for total protein levels and was corrected for background staining. Primary antibodies used were: Vps34 (#3358 and #4263, Cell Signaling), and SQSTM1/p62 (#8025, Cell Signaling).

siRNA knockdown

Silencing of ETV6-RUNX1 and Vps34 in REH cells or ETV6-RUNX1 transduced CB-

CD34⁺ cells was achieved by transfection of siRNAs with Dharmafect 4 (Thermo Scientific). 72 hours after transfection, cells were transfected again. Twenty-four hours after the second hit, cells were analyzed. The following siRNAs were used to silence ETV6-RUNX1: siETV6-RUNX1 #1: CCAUUGGGAGAAUAGCAGAAUGCAU; siETV6-RUNX1 #5: UGGGAGAAUAGCAGAAUGCAUACUU (7). Vps34 targeting siRNAs were purchased from Origene (Rockville, MD, USA).

Real-time PCR

RNA was extracted using Nucleospin RNA XS extraction columns according to manufacturer's protocol (Macherey-Nagel, Düren, Germany), upon which cDNA was synthesized. mRNA levels were quantified by incorporation of SYBR green (Thermo Scientific) during quantitative real-time PCR (Applied Biosystems 7900HT). Primers are described in supplementary methods.

Luciferase reporter assays

To study Vps34 promoter activity, a pEZX reporter construct consisting of a 1.4 kB region (-1383 to +58) of the Vps34 promoter upstream of the Gaussia luciferase gene (Genecopoeia, Rockville, MD, USA; HPRM12127) was used. The reporter construct was transfected in HEK293T cells together with the constructs of interest. In all experimental conditions, the amount of transfected DNA was equalized per backbone. At the end of the experiment, GFP expression was quantified in each sample by flow cytometric analysis and used to normalize luciferase activity. Constructs are described in supplementary methods.

MTT cytotoxicity assay

The sensitivity of ALL cell lines to hydroxychloroquine was analyzed using 3-(4,5-

dimethylthiazol-2-yl)-2,5-diphenyltetrazolium bromide (MTT) assay as described before (8). Cell survival was determined after 4 days of hydroxychloroquine exposure. Background signal was subtracted and experimental conditions are depicted as the percentage of signal compared to the untreated control.

Lentiviral knockdown of Vps34

Lentivirus was produced by transfecting HEK293T cells with second generation lentiviral helper vectors pPax2 (Addgene plasmid 12260) and VSV-G envelope (pMD2G; Addgene plasmid 12259) together with pLKO.1 Mission vector (Sigma) targeting *PIK3C3* (Vps34). Transfection was performed using XtremeGENE transfection reagent according to manufacturer's protocol (Promega, Madison, WI, USA). Target sequences used to silence *PIK3C3* were: GCTGCACAACAGACATTTGTA (shVps34#1; TRCN0000037798); GAGGCAAATATCCAGTTATAT (shVps34#2; TRCN0000196290); CCACGAGAGATCAGTTAAATA (shVps34#3; TRCN0000037794); GAGATGTACTTGAACGTAATG (shVps34#4; TRCN0000196840). Target sequence for used non-mammalian shRNA control vector was CAACAAGATGAAGAGCACCAA (NSC; SHC002). Virus was collected and concentrated by ultracentrifugation. For every experiment and every cell line, virus was titrated to obtain a transduction efficiency of 90%. This condition was equal to an MOI of 2.5. Cell lines were transduced using a spin-infection protocol. Cells were subsequently selected using the puromycin selection marker. A MACSQuant Analyzer (Miltenyi Biotec, Germany) was used to determine the number of viable, Propidium Iodide negative, cells.

Confocal laser scanning microscopy

Autophagy levels were visualized by the number and volume of LC3B positive vesicles. To quantify autophagy levels, confocal scanning microscopy was performed. REH cells were allowed to attach to a glass slide coated with 10 $\mu\text{g}/\text{mL}$ fibronectin (Sigma) for 30 minutes. Cells were subsequently fixated using 3% formaldehyde in PBS for 10 minutes at room temperature. After fixation, slides were blocked with 10% FCS and 0.2% goat serum in PBS and subsequently incubated overnight at 4°C with LC3B antibody (#2775, Cell Signaling). Slides were subsequently washed twice with PBS and stained with goat-anti-rabbit-Alexa 488 secondary antibody for 1 hour. After three PBS washes, slides were stained with DAPI (Sigma) for 5 minutes and mounted with ProLong Gold antifade reagent (Life Technologies). Images were acquired using a confocal laser scanning microscope (Leica SP5). Sequential scanning of different channels was performed at a resolution of 1024 x 1024 pixels in the x y plane and 0.15 μm steps in z -direction.

The system was equipped with a 63 \times plan-apochromat oil 1.4 NA DIC objective. The pinhole diameter was set to 1 airy unit (95.5 μm). DAPI and LC3B-anti-rabbit-Alexa 488 were excited with a 488-nm Argon laser and a 405-nm Diode-Pumped Solid-State laser, respectively. Fiji software was used for imaging processing. Brightness and contrast were optimized and applied to the entire image. Z-project using all slides and maximum intensity projection was used to show the number of LC3B-positive vesicles in Figure 4. For quantification of LC3B-positive vesicles, Z-stacks of images were deconvolved and processed using Huygens Professional software. Both the number and the average volume of vesicles were analyzed. For the quantification of number and volume of LC3B-positive vesicles, we excluded cells with atypical nuclei. For each experiment, LC3B-positive vesicles were quantified in at least 6 cells. 3D-deconvolved images shown in Fig. 3 were created using the same software.

Cell viability assays

Primary patient cells (1×10^6 cells) were co-cultured with or without primary mesenchymal stromal cells (5×10^4) for five days in a 24-well plate at 37 °C and 5% CO₂. Stromal cells were allowed to attach prior to the start of the experiment. Before the start of each experiment, leukemic cells were screened for CD19 positivity (Brilliant Violet 421 anti-human CD19 antibody). After five days of culture the percentage of viable leukemic cells was determined by flow cytometric analysis after staining with Brilliant Violet 421 anti-human CD19 antibody (Biolegend), FITC Annexin V (Biolegend), and Propidium Iodide (PI; Sigma). Primary leukemic cells were exposed to L-Asparaginase, Prednisolone or 6-Mercaptopurine in a concentration that was lethal to 50% of the patient derived leukemic cells (IC₅₀) as determined upfront by a 4-day MTT assay (1).

Primers used for real-time PCR

Primers for *ETV6-RUNX1* were 5'-TCGGGAAGACCTGGCTTACA-3' (forward) and 5'-TGGCATCGTGGACGTCTCTA-3' (reverse). Primers for *PIK3C3* (Vps34) were 5'-CCTGGAAGACCCAATGTTGAAG-3' (forward) and 5'-CGGGACCATACACATCCCAT-3' (reverse) or 5'-AGTTCCCGGTGTAGGTGGTA-3' (forward) and 5'-ACATTGGGTCTTCCAGGACA-3' (reverse). To normalize data, *HPRT* or *RPS20* were used as reference genes. Primers used were: *HPRT* 5'-TGACACTGGCAAAACAATGCA-3' (forward) and 5'-GGTCCTTTTCACCAGCAAGCT (reverse); *RPS20*: 5'-AAGGGCTGAGGATTTTTG-3' (forward) and 5'-CGTTGCGGCTTGTTAG-3' (reverse).

Constructs used for luciferase reporter assays

Constructs used were: pCMV5-RUNX1 (Addgene; plasmid 12426(9)); pCMV5-CBFβ

(Addgene; plasmid 12427(9)), pMSCV-ETV6-RUNX1 (a kind gift from Dr. Owen Williams, London, UK), pCMV6-XL5-HEY1 (Origene; plasmid SC115467), pcDNA3-EGR1 (Addgene; plasmid 11729(10)), pMT2-GATA1 (Addgene; plasmid 13626(11)), pFLAG-CMV2-GATA2 (Addgene; plasmid 1418(12)).

Statistical analysis

Statistical analysis of microarray data of paired (EV-eGFP⁺ versus ETV6-RUNX1-eGFP⁺) CB-CD34⁺ was performed using a linear mixed model in which multiple testing correction was applied by FDR (see also Material and Methods section on linear RNA amplification and gene expression profiling of CB-CD34⁺ cells). Microarray data of primary cells from ALL patients was normalized using vsnrma, batch effects were removed using the empirical Bayes method, and data were analyzed using LIMMA and FDR multiple testing correction.

Both the Student's t-test and the Student's paired t-test were used as statistical test when applicable. Bar graphs represent the mean of biological replicates. Error bars represent standard error of the mean (S.E.M.).

References

1. Den Boer ML, Harms DO, Pieters R, et al. Patient stratification based on prednisolone-vincristine-asparaginase resistance profiles in children with acute lymphoblastic leukemia. *J Clin Oncol.* 2003 Sep 1;21(17):3262-3268.
2. van den Berk LC, van der Veer A, Willems ME, et al. Disturbed CXCR4/CXCL12 axis in paediatric precursor B-cell acute lymphoblastic leukaemia. *Br J Haematol.* 2014 Jul;166(2):240-249.

3. Clement-Ziza M, Gentien D, Lyonnet S, Thierry JP, Besmond C, Decraene C. Evaluation of methods for amplification of picogram amounts of total RNA for whole genome expression profiling. *BMC Genomics*. 2009;10:246.
4. Bates D, Mächler M, Bolker B, Walker S. Fitting linear mixed-effects models using lme4. arXiv preprint arXiv:14065823. 2014.
5. van der Veer A, Waanders E, Pieters R, et al. Independent prognostic value of BCR-ABL1-like signature and IKZF1 deletion, but not high CRLF2 expression, in children with B-cell precursor ALL. *Blood*. 2013 Oct 10;122(15):2622-2629.
6. Petricoin EF, 3rd, Espina V, Araujo RP, et al. Phosphoprotein pathway mapping: Akt/mammalian target of rapamycin activation is negatively associated with childhood rhabdomyosarcoma survival. *Cancer Res*. 2007 Apr 1;67(7):3431-3440.
7. Zaliouva M, Madzo J, Cario G, Trka J. Revealing the role of TEL/AML1 for leukemic cell survival by RNAi-mediated silencing. *Leukemia*. 2011 Feb;25(2):313-320.
8. Pieters R, Loonen AH, Huismans DR, et al. In vitro drug sensitivity of cells from children with leukemia using the MTT assay with improved culture conditions. *Blood*. 1990 Dec 1;76(11):2327-2336.
9. Meyers S, Lenny N, Hiebert SW. The t(8;21) fusion protein interferes with AML-1B-dependent transcriptional activation. *Mol Cell Biol*. 1995 Apr;15(4):1974-1982.
10. Yu J, de Belle I, Liang H, Adamson ED. Coactivating factors p300 and CBP are transcriptionally crossregulated by Egr1 in prostate cells, leading to divergent responses. *Mol Cell*. 2004 Jul 2;15(1):83-94.
11. Monticelli S, Solymar DC, Rao A. Role of NFAT proteins in IL13 gene transcription in mast cells. *J Biol Chem*. 2004 Aug 27;279(35):36210-36218.

12. Tong Q, Tsai J, Tan G, Dalgin G, Hotamisligil GS. Interaction between GATA and the C/EBP family of transcription factors is critical in GATA-mediated suppression of adipocyte differentiation. *Mol Cell Biol.* 2005 Jan;25(2):706-715.

SUPPLEMENTARY FIGURE LEGENDS

Supplementary Figure S1. Ectopic expression of ETV6-RUNX1 in healthy

CD34⁺ progenitors activates pro-proliferative and pro-survival transcriptional networks

To generate retrovirus, bicistronic retroviral DNA constructs were used co-expressing ETV6-RUNX1 and eGFP. CD34-positive hematopoietic progenitors (CB-CD34⁺ cells) were isolated from cord blood, upon which cells were divided in two fractions. One fraction was transduced with ETV6-RUNX1-IRES-eGFP, while the other fraction was transduced with control EV-IRES-eGFP (n = 5 biological replicates). Forty hours after transduction, CD34⁺ DAPI⁻ eGFP⁺ hematopoietic progenitors were sorted (for gating strategy see supplementary Figure 1). After sorting, RNA was extracted, checked for quality and linearly amplified. Gene expression analysis was subsequently performed using Affymetrix Genechip microarrays.

(A) Flowchart of the experimental approach.

(B) Heat map displaying gene probe sets that were either over-expressed (in red) or under-expressed (in blue) in comparison to the mean expression of all probe sets. Forty hours after transduction, 196 gene probe sets were significantly ($p \leq 0.05$; FDR-adjusted) over-expressed or under-expressed in ETV6-RUNX1 positive CB-CD34⁺ cells in comparison to control CB-CD34⁺ cells. Data were analyzed using a linear mixed model. Genes were considered differentially expressed when $p \leq 0.05$ after multiple testing correction using false discovery rate (FDR).

(C) Ingenuity pathway analysis of the differentially expressed genes was performed to elucidate the interconnected transcriptional network present within this gene set. The level of up- (red) and down-regulation (blue) of genes was visualized by the intensity of the colors. Direct relationships were marked with undotted arrows. Indirect relationships were marked with dotted arrows.

(D-E) Ingenuity pathway analysis was used to analyze gene ontology (GO) functional categories and activation of disease/function annotation based on current literature. Functional categories inducing a pro-survival or a pro-proliferative state in ETV6-RUNX1-positive HPCs and the differentially regulated genes responsible for this prediction are shown.

Supplementary Figure S2. Pathway analysis of ETV6-RUNX1 positive CD34+ hematopoietic progenitors.

(A) Ingenuity pathway analysis was used to analyze gene ontology (GO) functional categories and activation of disease/ function annotation based on current literature. Significantly regulated functional categories are listed with their p-value (right-tailed Fisher Exact Test after Benjamini-Hochberg multiple testing correction) and regulation Z-score. This analysis reflect the pathways induced in CB-CD34+ cells by ETV6-RUNX1 40 hours after transduction

(B) Schematic representation of differentially regulated genes predicted to induce cellular homeostasis.

(C) Ingenuity pathway analysis was used to analyze gene ontology (GO) functional categories and activation of disease/function annotation based on current literature. Table shows annotations that were similarly activated in ETV6-RUNX1 positive BCP-ALL patients and ETV6-RUNX1 positive CB-CD34⁺ cells (40 hours after transduction). The top 500 differentially expressed genes between ETV6-RUNX1 positive and EVT6-RUNX1 negative patients in the Erasmus MC cohort were used for this analysis.

Supplementary Figure S3. Vps34 is recurrently up-regulated in ETV6-RUNX1 positive BCP-ALL.

We compared gene expression levels in ETV6-RUNX1 positive ALL cells with gene expression levels in ETV6-RUNX1 negative ALL cells. We used 5 cohorts in which ETV6-RUNX1 positive BCP-ALL patients were included and gene expression data were publically available. In addition, we analyzed differential gene expression in an ETV6-RUNX1 knockdown study performed in an ETV6-RUNX1 positive leukemic cell line. “Yes” represents the differential expression of the gene in the particular study. “No” represents no differential expression of the gene in the study. “?” represents unavailable data.

Supplementary Figure S4. Early effects of ETV6-RUNX1 expression in CB-CD34+ cells

(A) Flow chart used to study the early effects of ETV6-RUNX1 fusion protein expression in cord blood-derived CD34-positive hematopoietic progenitors (CB-CD34+ cells). CB-CD34+ cells were isolated from cord blood. Per cord blood donor, cells were divided in two fractions of which one was transduced with ETV6-RUNX1-IRES-GFP and the other fraction with control EV-IRES-GFP. Viable transduced HPCs were sorted after 20 hours based on DAPI negativity and CD34 and GFP positivity. RNA was extracted from sorted CB-CD34+ cells, controlled for quality and linearly amplified after which gene expression analysis was performed with Affymetrix GeneChip Human Genome U133 Plus 2.0 microarrays.

(B) Graphs showing the gating strategy used to sort alive, CD34-positive, transduced cord blood cells. First living cells were gated based on FSC, SSC and the absence of DAPI incorporation. CD34-positive cells were selected based on the positive expression compared to an isotype control. Finally, CD34-positive transduced cells were sorted based on eGFP expression. Post-sort purity was more than 95%.

(C) Graph showing gene expression levels of *ETV6-RUNX1* relative to housekeeping gene RPS20 quantified with Q-PCR (n = 5). EV represents levels in CB-CD34+ cells transduced

with the empty vector control. ETV6-RUNX1 represents levels in CB-CD34+ cells transduced with the ETV6-RUNX1 vector. Data are means \pm SEM; *** $p \leq 0.001$.

(D) Heat map showing which gene probe sets are relatively over-expressed (in red) and which gene probe sets are relatively under-expressed (in blue) compared to the mean expression of all differentially regulated gene probe sets. 203 gene probe sets were significantly ($p \leq 0.05$; FDR-adjusted) over-expressed or under-expressed when ETV6-RUNX1 positive HPCs were compared to control HPCs 20 hours after transduction.

Supplementary Figure S5. Vps34 expression in ETV6-RUNX1 positive cells

(A) Graph showing the 2log expression (at initial diagnosis) of the gene probe set mapped to Vps34 in a cohort of 98 pediatric ALL patients that eventually relapsed after treatment (relapsed patients in the Erasmus MC cohort). Grey dashed line represents mean expression of all patients. Gene expression of ETV6-RUNX1 positive patients was compared to gene expression of all other B-ALL patients (excluding T-ALL): *** FDR-adjusted $p = 5.11 \times 10^{-6}$.

(B) Graph showing gene expression of ETV6-RUNX1 after knockdown of the ETV6-RUNX1 fusion protein. mRNA levels were determined in REH (n=2) and ETV6-RUNX1 transduced CB-CD34+ cells (n=1) by Q-PCR, normalized to HPRT, and compared to the average expression of cells transfected with scrambled control siRNAs (n = 3, $p \leq 0.05$).

Supplementary Figure S6. Autophagy levels are high in ETV6-RUNX1 positive BCP-ALL cells

(A) Western blot analysis of proteins important in the autophagy pathway, namely Vps34, p62 (sequestosome 1), and LC3B in primary patient BCP-ALL cells (n=5 for ETV6-RUNX1 positive BCP-ALL patients; n=6 for ETV6-RUNX1 negative BCP-ALL patients).

(B) Quantification of experiment performed in (A). Protein expression of Vps34 and p62 is relative to actin expression.

(C) Quantification of protein levels of Vps34 measured by reverse phase protein array (RPPA) in 10 normal bone marrow samples (nBM), 30 ETV6-RUNX1 positive primary BCP-ALL patient samples (ETV6-RUNX1+), and 29 B-Other primary BCP-ALL patient samples (BO). Data are means \pm S.E.M.; * $p \leq 0.05$, *** $p \leq 0.001$.

(D) Representative confocal images of REH cells after permeabilization and staining with DAPI and LC3B antibody. Z-stacks were deconvolved using Huygens Professional software, after which number and volume of LC3B-positive vesicles could be quantified.

Supplementary Figure S7. Vps34 is essential for the survival of ETV6-RUNX1 positive leukemic cells

(A) ETV6-RUNX1-positive (REH and REHS1) and ETV6-RUNX1-negative (NALM6) BCP-ALL cells were lentivirally transduced with scrambled shRNA control (NSC) or two distinct Vps34 shRNA constructs. NI represents non-infected cells. Cells were cultured for 18 days. To determine the effect on proliferation, cell counts were performed every 2-3 days. The average increase in cell numbers per day. T-test was performed to compare control conditions (NSC) with Vps34 knockdown conditions ($n = 3$, ** $p \leq 0.01$, *** $p \leq 0.001$). Error bars represent S.E.M.

(B) ETV6-RUNX1-positive (REH) BCP-ALL cells were lentivirally transduced with scrambled shRNA control (NSC) or two distinct shRNA constructs to silence Vps34 expression. After 7 days of culture, flow cytometrical analysis was performed to determine the effect of Vps34 knockdown on survival and cell cycle progression. Representative FACS plots are shown ($n = 3$).

(C) Schematic representation of the different transcript variants of Vps34, based on currently available literature (Ensembl Genome Browser; ENSG00000078142) and the binding locations of shVps34#1-shVps34#4.

(D) Representative western blot showing the knockdown of Vps34 in REH cells.

(E-F) ETV6-RUNX1-positive (REH and REHS1) and ETV6-RUNX1-negative (NALM6)

BCP-ALL cells were lentivirally transduced with scrambled shRNA control (NSC, black) or two distinct Vps34 shRNA constructs (grey; shVps34 #3 and shVps34#4). NI represents non-infected cells. Cells were cultured for 18 days. To determine the effect on proliferation, cell counts were performed every 2-3 days. Representative graphs are shown **(E)**. The average increase in cell numbers per day is shown in **(F)**. T-test was performed to compare control conditions (NSC) with Vps34 knockdown conditions ($n = 3$, ** $p \leq 0.01$, *** $p \leq 0.001$). Error bars represent S.E.M.

(G-H) ETV6-RUNX1-positive (REH) BCP-ALL cells were lentivirally transduced with scrambled shRNA control (NSC) or two distinct shRNA constructs to silence Vps34 expression. After 7 days of culture, flow cytometrical analysis was performed to determine the effect of Vps34 knockdown on survival and cell cycle progression. The percentage of viable (AnnexinV positive, Propidium Iodide negative), actively cycling cells was determined using DyeCycle. Data were depicted as the percentage of cells in active cell cycle (S, G2, M stage) at day 7 after transduction ($n = 2$, * $p \leq 0.05$) **(G)**. The percentages of early apoptotic (AnnexinV positive, Propidium Iodide negative) and late apoptotic (Propidium Iodide positive) cells were determined 7 days after transduction ($n = 2$, * $p \leq 0.05$, *** $p \leq 0.001$) **(H)**. Error bars represent S.E.M.

Supplementary Figure S8. ETV6-RUNX1 positive ALL cells are relatively sensitive to treatment with hydroxychloroquine

(A) Bar graph showing the cell viability of HCQ-treated conditions (10 $\mu\text{g/ml}$) compared to HCQ-untreated conditions after 4 days (MTT). Green bars represent ETV6-RUNX1 positive

BCP-ALL cell lines. Black bars represent ETV6-RUNX1 negative BCP-ALL cell lines. Dark grey bars represent T-ALL cell lines.

(B) Calculation of IC₅₀ concentrations of two ETV6-RUNX1-positive ALL cell lines (green), and two ETV6-RUNX1-negative ALL cell lines (black and gray). n = 4, *** p ≤ 0.001. IC₅₀ values for Jurkat cells were not reached during treatment with 40 µg/ml HCQ (the highest concentration used in this assay).

(C) Flow cytometrical gating strategy used to analyze survival after HCQ treatment of primary BCP-ALL patient samples in co-culture. First, forward and sideward scatter were used to gate living and apoptotic events. Second, primary mesenchymal stromal cells (MSCs) were gated out based on CD19-expression and autofluorescence in the Amcyan channel (events in red gate were excluded from analysis). Then, viable cells were gated based on Annexin-V and Propidium Iodide staining and subsequently based on CD19-expression. Percentage of living cells was calculated by dividing the number of AnnexinV negative, PI negative, CD19 positive events by the number of events after gating out the MSCs.

(D) Graph showing relative survival of primary ETV6-RUNX1 negative BCP-ALL cells after treatment with increasing concentrations of HCQ compared to untreated controls. Light grey bars represent treatment with 5 µg/ml HCQ. Grey bars represent treatment with 10 µg/ml HCQ. Experiment was performed in absence and presence of primary MSCs (n=3 for conditions in absence of MSCs, n = 5 for conditions in presence of MSCs).

Supplementary Figure S9. Autophagy inhibition sensitizes ETV6-RUNX1 positive BCP-ALL

(A) Primary ETV6-RUNX1-positive BCP-ALL cells were cultured in absence or presence of IC-50 concentrations of L-Asparaginase and increasing concentrations of HCQ. Flow cytometric analysis was performed to determine the percentage of non-apoptotic (Annexin V negative, Propidium Iodide negative, CD19 positive) cells (for gating strategy see

supplementary Figure 6d). First, the survival of primary leukemic blasts in presence of L-Asparaginase was compared to their survival in absence of L-Asparaginase (see supplementary Figure 7a for the effect of asparaginase in the absence of treatment with other effectors). Next, data was depicted as fold reduction compared to HCQ-untreated controls.

(B) Primary ETV6-RUNX1-positive BCP-ALL cells were co-cultured with primary MSCs in absence or presence of IC-50 concentrations of L-Asparaginase and increasing concentrations of HCQ. Flow cytometric analysis was performed to determine the percentage of non-apoptotic cells. The survival of primary leukemic blasts in presence of L-Asparaginase was compared to their survival in absence of L-Asparaginase. Next, data from individual patients was depicted as fold reduction compared to HCQ-untreated controls. Light grey bars represent treatment with 5 $\mu\text{g/ml}$ HCQ. Grey bars represent treatment with 10 $\mu\text{g/ml}$ HCQ. Dark grey bars represent treatment with 20 $\mu\text{g/ml}$ HCQ. Experiment was performed twice with cells of patients #1 and #2.

(C) Co-culture experiments were performed with primary ETV6-RUNX1 positive BCP-ALL cells and MSCs. Cells were cultured in presence or absence of L-Asparaginase and increasing concentrations of HCQ. Flow cytometric analysis was performed to determine the percentage of non-apoptotic cells. The survival of primary leukemic blasts in presence of L-Asparaginase was compared to their survival in absence of L-Asparaginase. Next, data from individual patients was depicted as fold reduction compared to HCQ-untreated controls. Data were depicted as fold reduction compared to HCQ-untreated controls (n=4 for HCQ 2.5 $\mu\text{g/ml}$; n = 5 for HCQ 5 $\mu\text{g/ml}$ and 10 $\mu\text{g/ml}$; n=3 for HCQ 20 $\mu\text{g/ml}$).

(D) Co-culture experiments were performed with primary ETV6-RUNX1 negative BCP-ALL cells and MSCs. Cells were cultured in presence or absence of L-Asparaginase and increasing concentrations of HCQ. Flow cytometric analysis was performed to determine the percentage of non-apoptotic cells. The survival of primary leukemic blasts in presence of L-Asparaginase

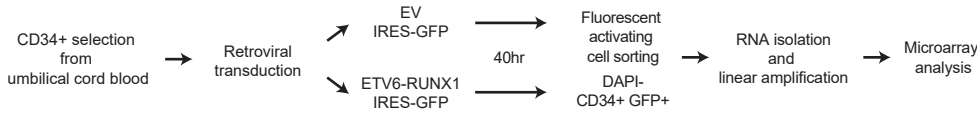
was compared to their survival in absence of L-Asparaginase. Next, data was depicted as fold reduction compared to HCQ-untreated controls (n = 3 for conditions in absence of MSCs, n = 5 for conditions in presence of MSCs).

(E/F) Co-culture experiments were performed with primary ETV6-RUNX1 positive BCP-ALL cells and MSCs. Cells were cultured in presence or absence of Prednisolone (**E**) or 6-Mercaptopurine (**F**) and increasing concentrations of HCQ. Flow cytometric analysis was performed to determine the percentage of non-apoptotic (Annexin V negative, Propidium Iodide negative, CD19 positive) cells. The survival of primary leukemic blasts in presence of Prednisolone (**E**) or 6-Mercaptopurine (**F**) was compared to their survival in absence of these drugs. Next, data was depicted as fold reduction compared to HCQ-untreated controls (n = 5 for conditions in absence of MSCs, n = 7 for conditions in presence of MSCs for **(E)**, n = 4 for conditions in absence of MSCs, n = 4 for conditions in presence of MSCs for **(F)**).

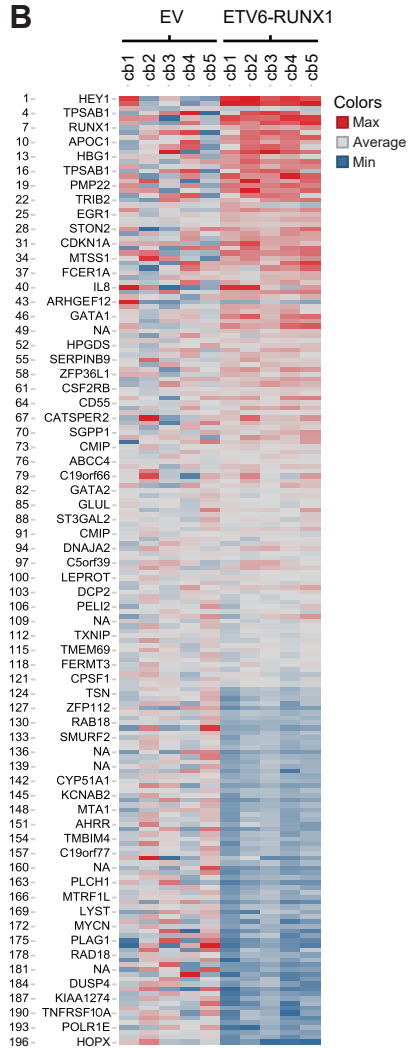
Error bars represent S.E.M.

Supplementary Figure S1. Ectopic expression of ETV6-RUNX1 in healthy CD34+ progenitors activates pro-proliferative and pro-survival transcriptional networks

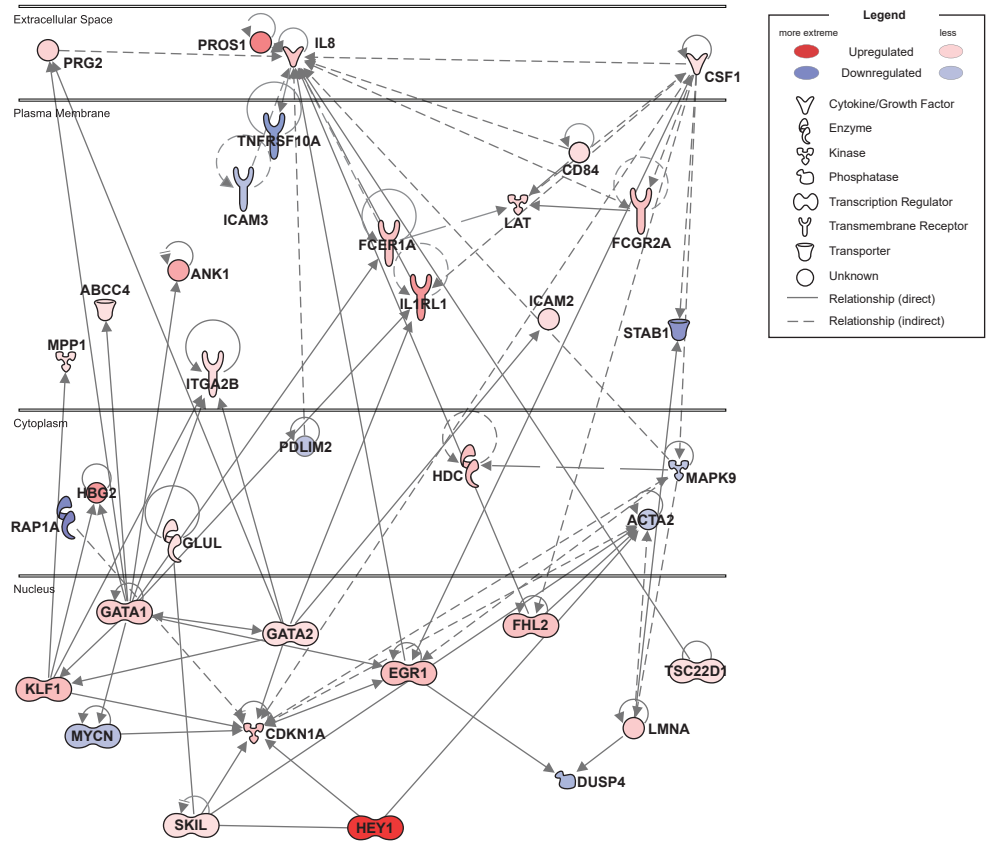
A



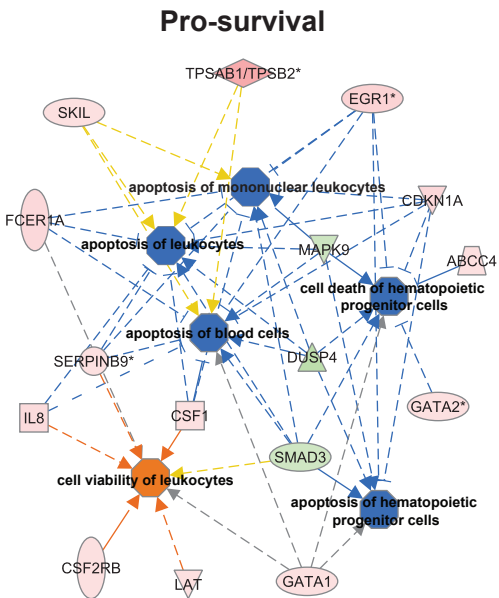
B



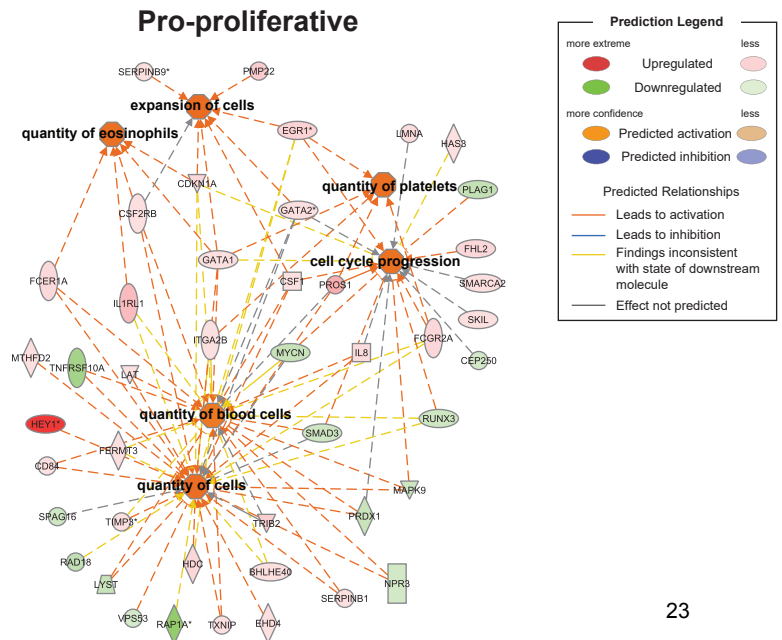
C



D



E

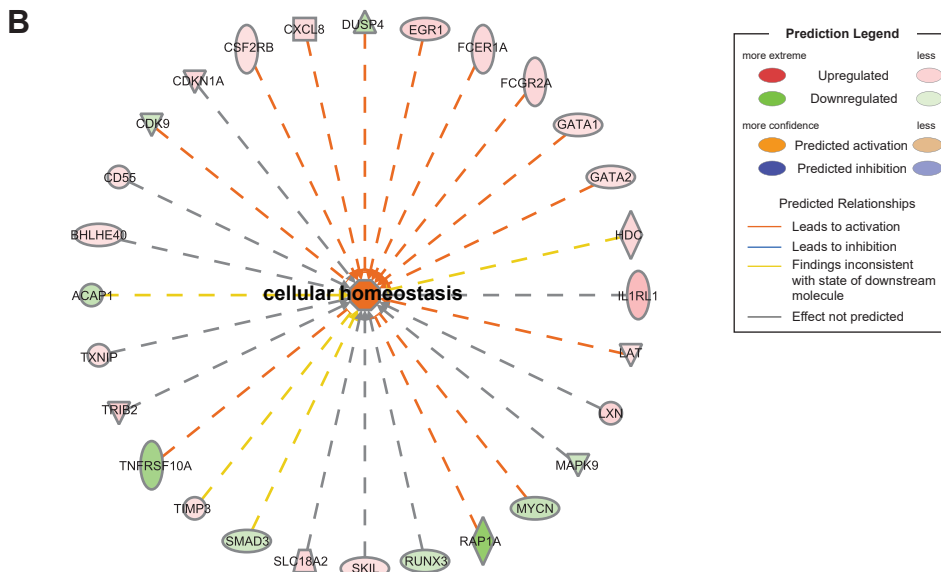


Supplementary Figure S2. Pathway analysis of ETV6-RUNX1 positive CD34+ hematopoietic progenitors

A

Diseases or Functions Annotation	p-Value	Activation z-score	Activation Z-score
survival of organism	3,93E-02	3,221	
production of reactive oxygen species	4,49E-02	2,979	
organization of cytoplasm	4,49E-02	2,612	
expansion of cells	4,49E-02	2,578	
quantity of cells	2,19E-03	2,554	
differentiation of bone marrow cells	2,56E-02	2,412	
degranulation of phagocytes	3,05E-03	2,355	
cellular homeostasis	1,43E-02	2,297	
aggregation of cells	1,51E-02	2,206	
differentiation of HPCs	2,42E-02	2,187	
quantity of blood platelets	4,49E-02	2,169	
quantity of eosinophils	2,92E-02	2,125	
binding of cells	9,47E-03	2,118	
cell cycle progression	3,73E-02	2,042	
engulfment of cells	2,19E-02	2,024	
recruitment of leukocytes	2,44E-03	2,021	
response of granulocytes	2,19E-02	2,000	
fibrosis	4,49E-02	-2,126	
apoptosis of hematopoietic progenitor cells	4,49E-02	-2,183	
cell death of hematopoietic progenitor cells	1,70E-02	-2,211	
inflammation of liver	1,51E-02	-2,236	
apoptosis of blood cells	3,69E-02	-2,349	
apoptosis of leukocytes	4,49E-02	-2,369	
apoptosis of mononuclear leukocytes	4,49E-02	-2,401	
hypertrophy of heart	4,49E-02	-2,425	
organismal death	1,63E-03	-2,601	

Colors
■ 3,22
■ 0.00
■ -2,60



C **Pathway analysis of ETV6-RUNX1 positive CB-CD34+ and patients**

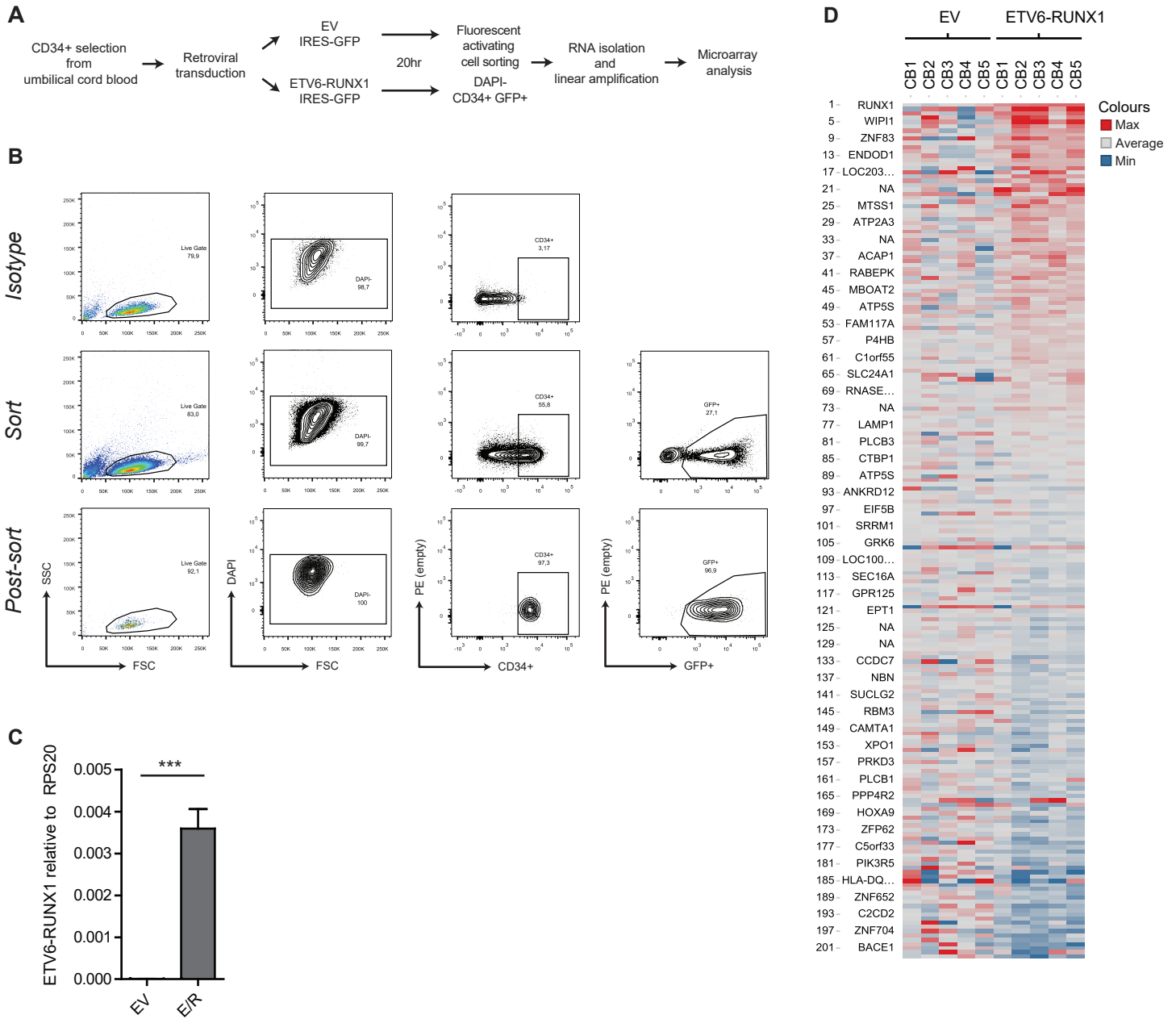
Disease or functions Annotation (GO)	CB-CD34	Top500	Activation Z-score	CB-CD34	Top500
Organismal death	-5.16	-5.16		p = 0.00163	p = 0.00553
Quantity of cells	2.75	2.75		p = 0.00219	p = 0.0522
Cellular homeostasis	2.75	2.75		p = 0.0143	p = 0.0946
Cell viability	2.75	2.75		p = 0.0135	p = 0.00816
Organization of cytoskeleton	2.75	2.75		p = 0.0449	p = 0.0214
Apoptosis of leukocytes	-5.16	-5.16		p = 0.0449	p = 0.150
Aggregation of cells	2.75	2.75		p = 0.0151	p = 0.150
Quantity of blood cells	2.75	2.75		p = 0.000202	p = 0.0404
Cell viability of leukocytes	2.75	2.75		p = 0.0308	p = 0.150
Quantity of leukocytes	2.75	2.75		p = 0.000930	p = 0.0517

Colours
■ 2.75
■ 0.00
■ -5.16

Supplementary Figure S3. Vps34 is recurrently up-regulated in ETV6-RUNX1 positive BCP-ALL.

Gene Symbol	Patient cohorts					shRNA-KD E-R
	Yeoh	Den Boer	Gandemer	Andersson	Fine	Fuka
	Cancer Cell 2002	Lancet Onc 2009	BMC Gen 2007	PNAS 2005	Blood 2004	PLoSOne, 2011
PIK3C3 (Vps34)	yes	yes	yes	yes	?	yes
TCFL5	yes	yes	yes	no	yes	no
EPOR	yes	yes	no	no	yes	no
TUSC3	yes	yes	no	yes	?	no
ARHGEF4	yes	yes	yes	no	?	yes
TNFRSF21	yes	yes	no	yes	?	yes
ABHD3	yes	yes	no	yes	?	no
FCHSD2	yes	yes	no	yes	?	no
NOVA1	yes	yes	no	yes	?	no
IDI1	yes	yes	no	yes	?	no
KCNN1	yes	yes	no	no	?	no
CLIC5	yes	yes	no	no	?	no
TNS1	yes	yes	no	no	?	no
BIRC7	yes	yes	no	no	?	no

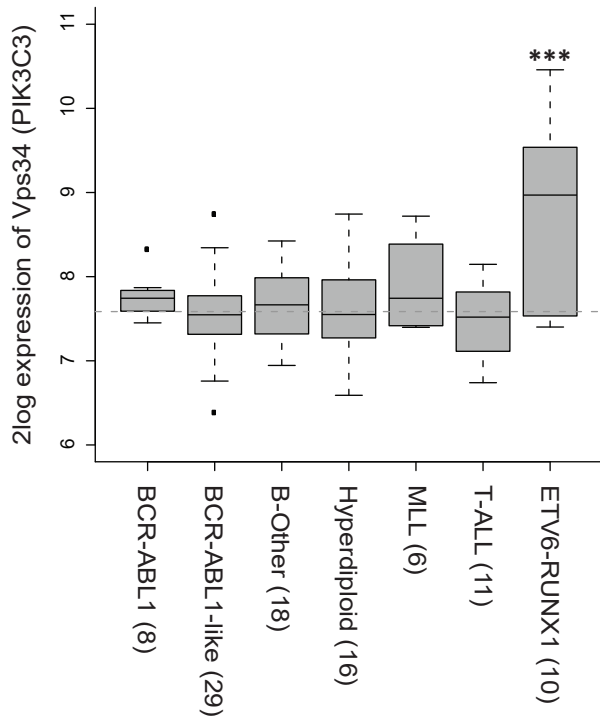
Supplementary Figure S4. Early effects of ETV6-RUNX1 expression in cord blood-derived CD34+ progenitors



Supplementary Figure S5. Vps34 expression in ETV6-RUNX1 positive cells

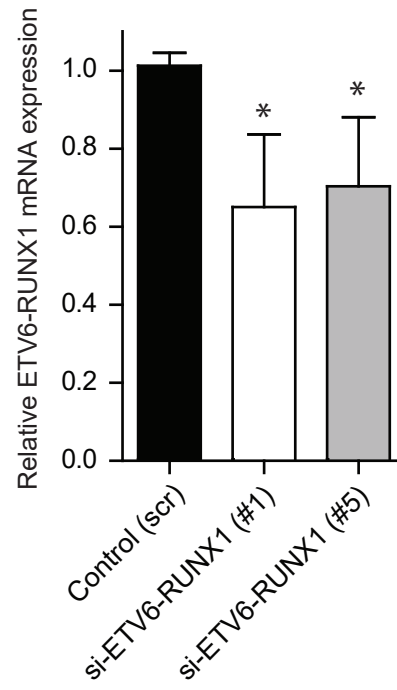
A

Relapsed ALL (n = 98)



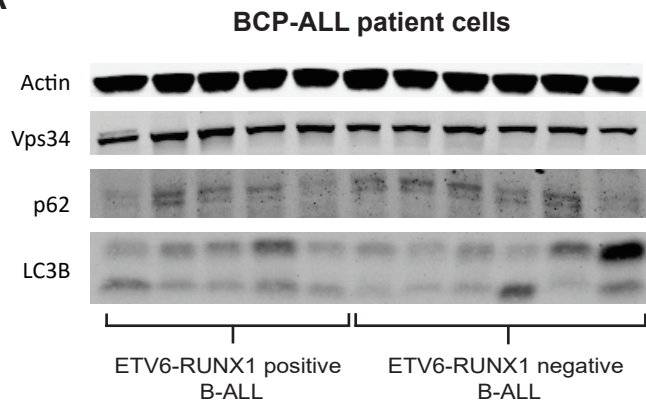
B

SiRNA KD (E-R+)

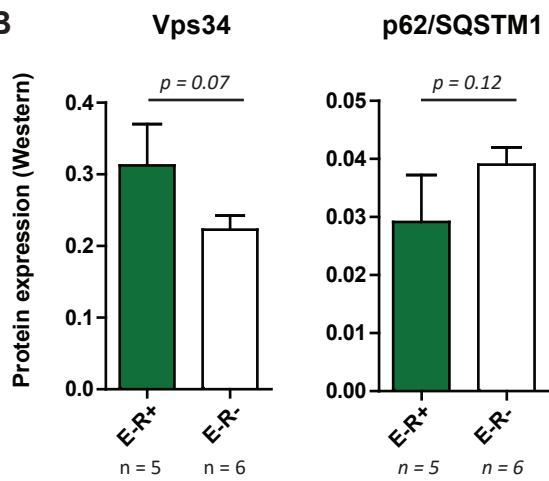


Supplementary Figure S6. Autophagy levels are high in ETV6-RUNX1 positive BCP-ALL cells

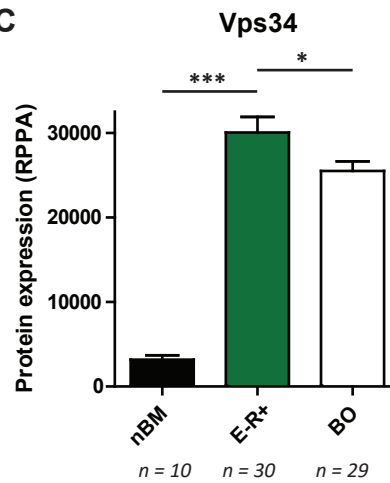
A



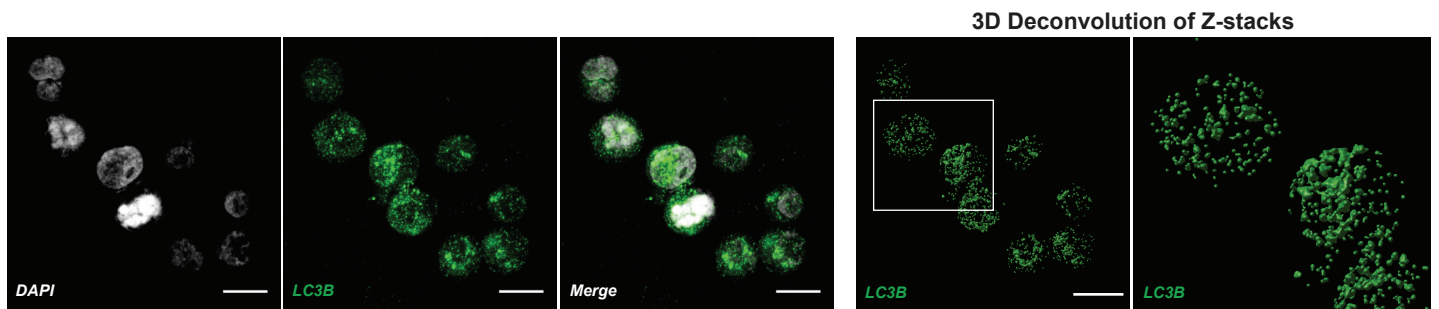
B



C

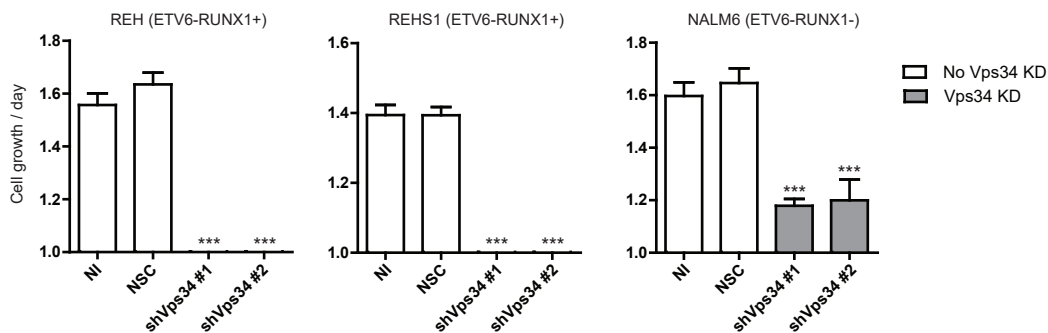


D

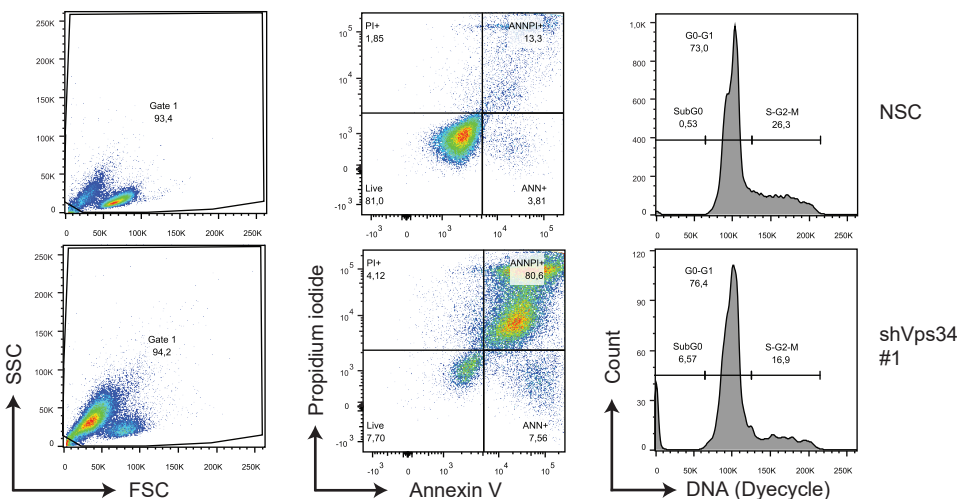


Supplementary Figure S7. Vps34 is essential for the survival of ETV6-RUNX1 positive leukemic cells

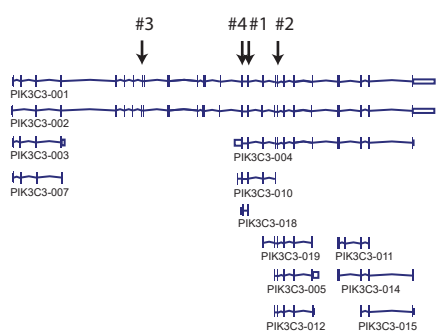
A



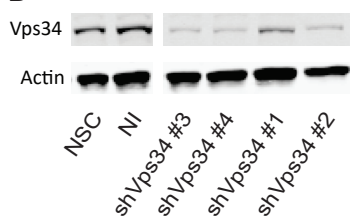
B



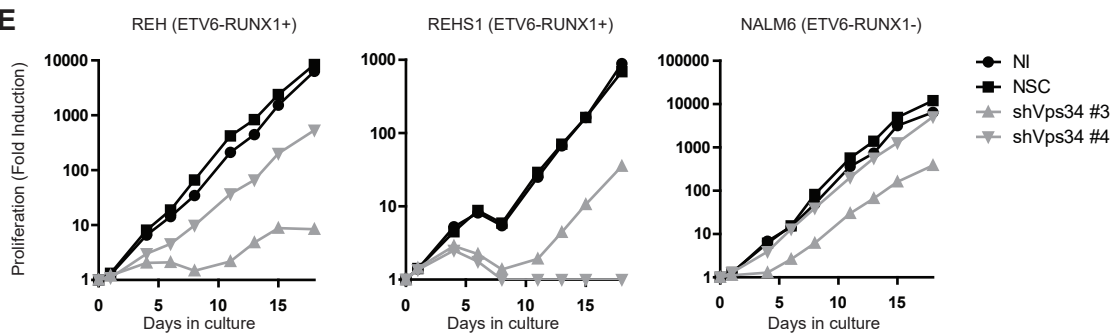
C



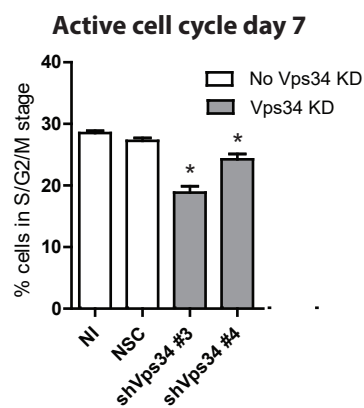
D



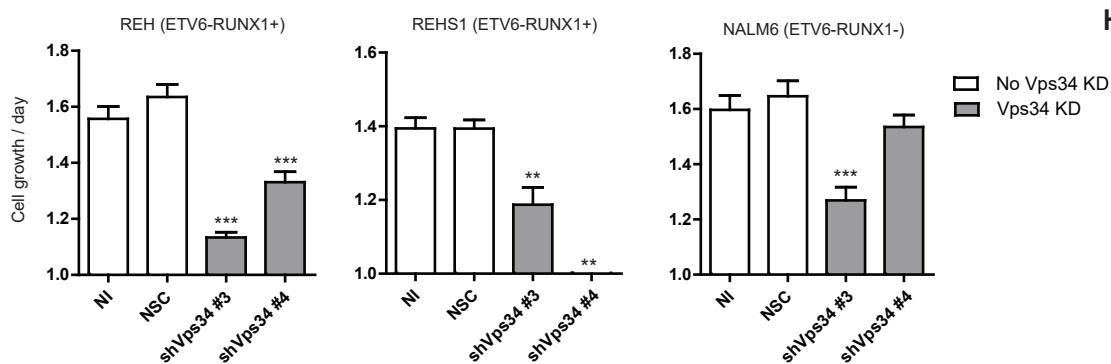
E



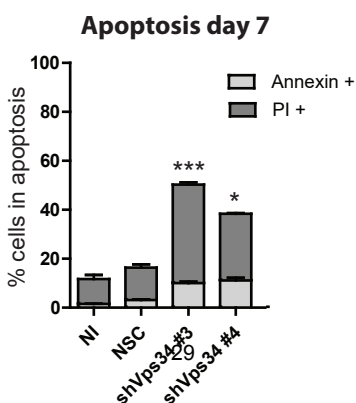
G



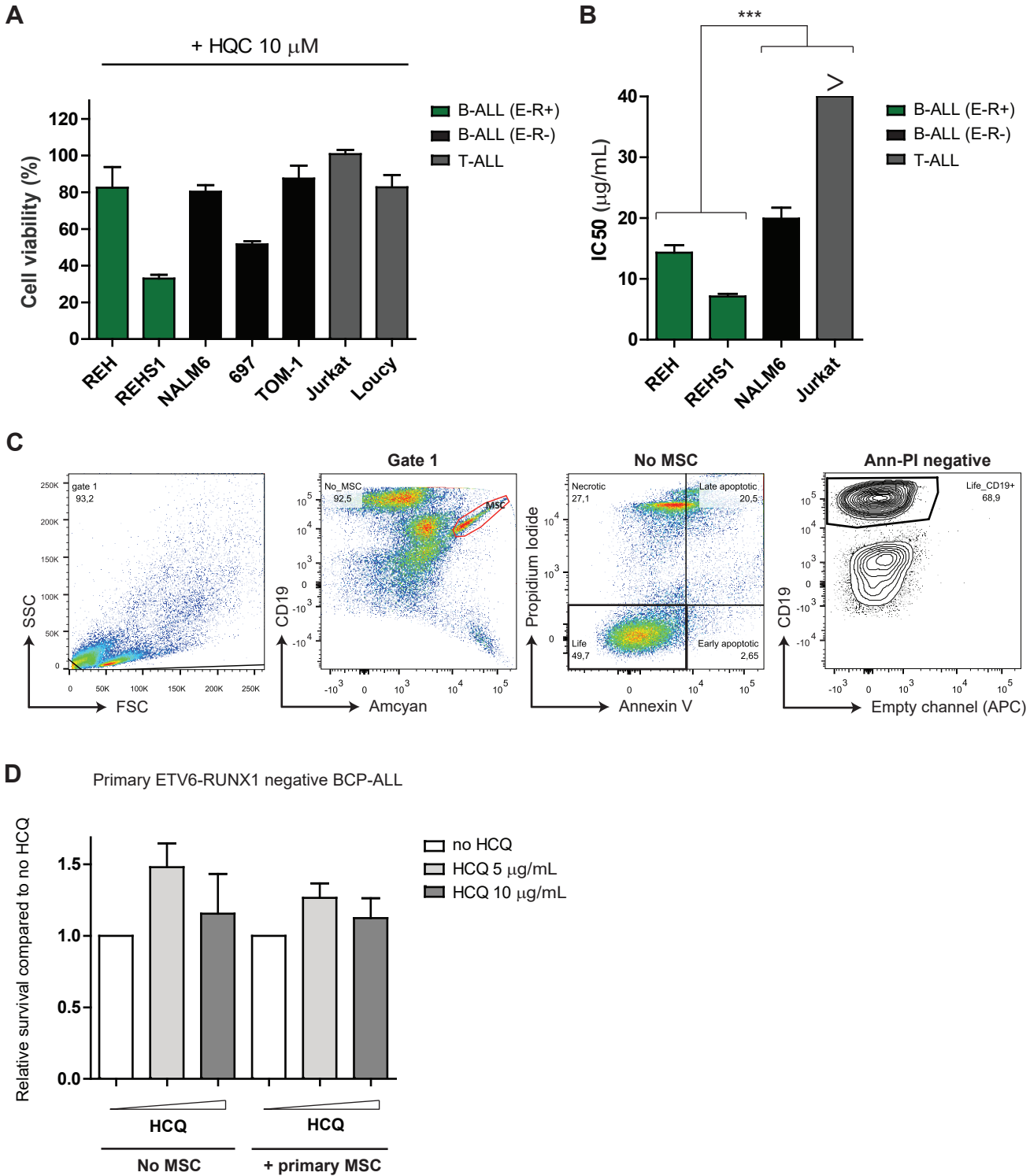
F



H

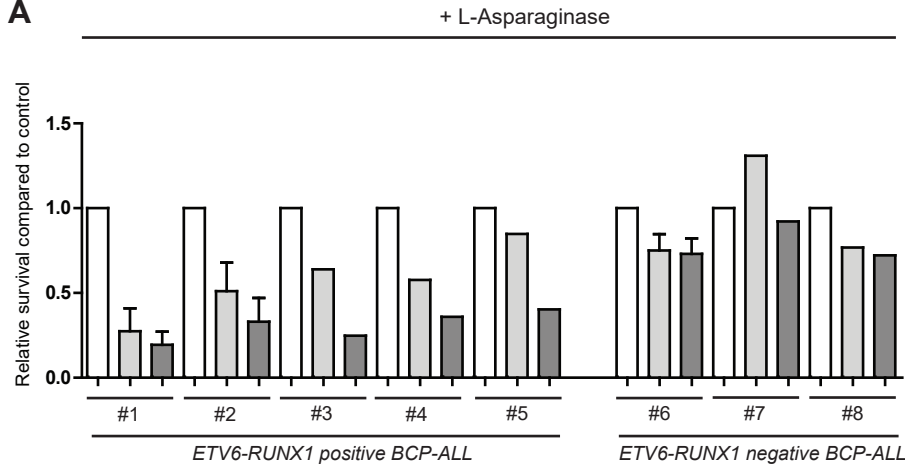


Supplementary Figure S8. ETV6-RUNX1 negative ALL cells are not sensitive to treatment with hydroxychloroquine

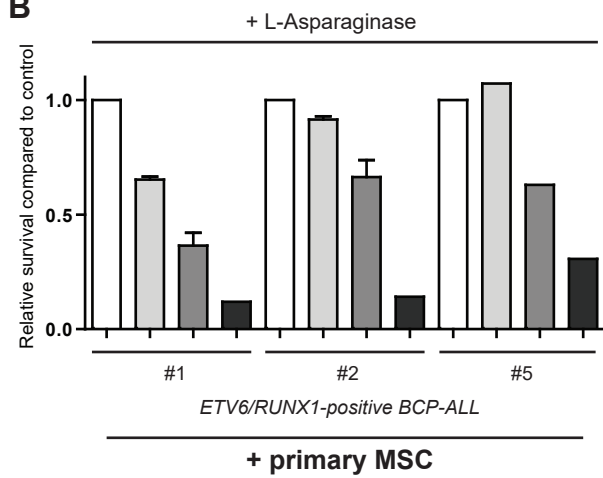


Supplementary Figure S9. Autophagy inhibition sensitizes ETV6-RUNX1 positive BCP-ALL to L-Asparaginase

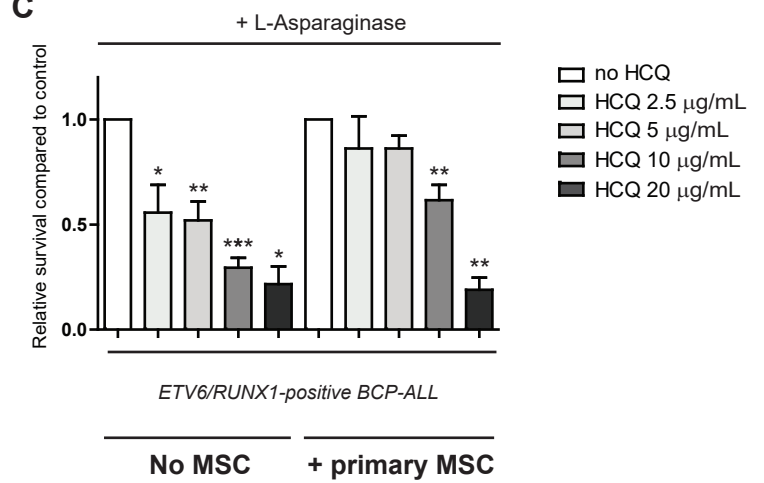
A



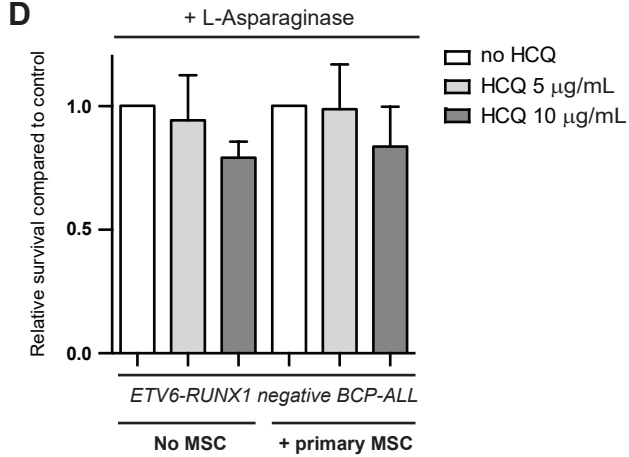
B



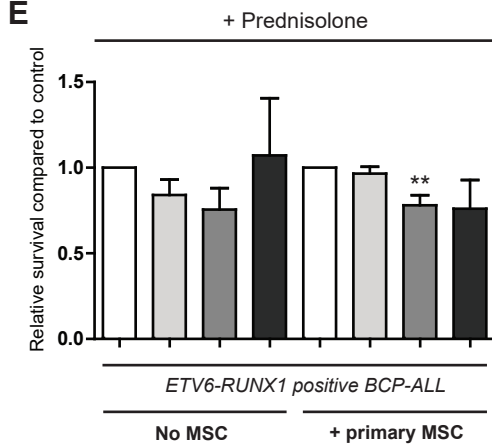
C



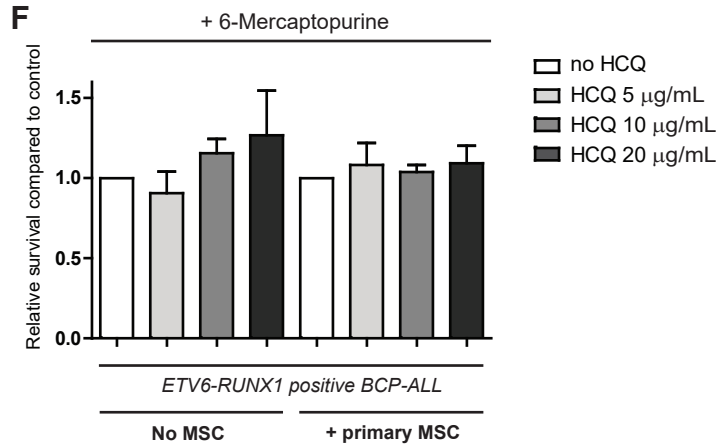
D



E



F



Supplementary Table 1. Differentially regulated genes in ETV6-RUNX1 positive primary leukemic cells

Probe.ID	Chr	Chr.band	Gene.Symbol	Gene.Name	logFC	AveExpr	t	P.Value	adj.P.Val
206231_at	19	19p13.1	KCNN1	potassium intermediate/small conductance calcium-activated ch	2,77	7,49	43,45	1,08E-183	5,92E-179
227377_at	17	17q21.32	IGF2BP1	insulin-like growth factor 2 mRNA binding protein 1	2,11	6,74	36,96	5,87E-154	1,61E-149
213317_at	6	6p21.1-p12.1	CLIC5	chloride intracellular channel 5	4,23	5,38	35,93	5,11E-149	9,30E-145
210683_at	19	19p13.3	NRTN	neurturin	3,05	6,15	35,45	1,01E-146	1,38E-142
226817_at	18	18q12.1	DSC2	desmocollin 2	1,95	6,77	33,23	6,96E-136	7,61E-132
213423_x_at	8	8p22	TUSC3	tumor suppressor candidate 3	2,37	5,75	33,02	8,18E-135	7,45E-131
237206_at	17	17p11.2	MYOCD	myocardin	2,60	5,91	32,86	4,74E-134	3,71E-130
206032_at	18	18q12.1	DSC3	desmocollin 3	2,55	5,92	32,69	3,28E-133	2,24E-129
209962_at	19	19p13.3-p13.2	EPOR	erythropoietin receptor	1,64	6,32	32,68	3,78E-133	2,30E-129
206033_s_at	18	18q12.1	DSC3	desmocollin 3	2,44	5,43	32,60	9,81E-133	5,36E-129
220451_s_at	20	20q13.3	BIRC7	baculoviral IAP repeat-containing 7	1,12	7,10	32,43	6,40E-132	3,18E-128
37986_at	19	19p13.3-p13.2	EPOR	erythropoietin receptor	1,03	5,91	32,02	7,42E-130	3,38E-126
219866_at	6	6p21.1-p12.1	CLIC5	chloride intracellular channel 5	1,89	6,74	31,85	5,05E-129	2,12E-125
215054_at	19	19p13.3-p13.2	EPOR	erythropoietin receptor	1,58	6,77	31,01	8,28E-125	3,24E-121
238532_at	14	14q24.3-q31.1	DPF3	D4, zinc and double PHD fingers, family 3	2,19	6,10	30,79	1,07E-123	3,89E-120
1552519_at	2	2q24.1	ACVR1C	activin A receptor, type IC	1,93	6,09	30,47	4,52E-122	1,54E-118
205109_s_at	2	2q22	ARHGEF4	Rho guanine nucleotide exchange factor (GEF) 4	2,34	6,51	30,19	1,21E-120	3,88E-117
209228_x_at	8	8p22	TUSC3	tumor suppressor candidate 3	1,55	6,02	30,11	2,99E-120	9,09E-117
221747_at	2	2q35-q36	TNS1	tensin 1	1,25	6,75	29,71	3,46E-118	9,95E-115
203464_s_at	17	17p11.2	EPN2	epsin 2	0,60	6,81	29,60	1,26E-117	3,43E-114
1556511_a_at	NA	NA	---	---	2,19	6,08	28,74	3,17E-113	8,26E-110
236442_at	14	14q24.3-q31.1	DPF3	D4, zinc and double PHD fingers, family 3	1,58	5,95	28,30	5,25E-111	1,31E-107
238727_at	2	2q36.1	---	---	1,38	4,67	28,22	1,36E-110	3,24E-107
218864_at	2	2q35-q36	TNS1	tensin 1	1,13	6,38	27,95	3,55E-109	8,10E-106
209963_s_at	19	19p13.3-p13.2	EPOR	erythropoietin receptor	0,73	6,37	27,93	4,26E-109	9,32E-106
243917_at	6	6p21.1-p12.1	CLIC5	chloride intracellular channel 5	1,19	6,34	27,90	6,18E-109	1,30E-105
221748_s_at	2	2q35-q36	TNS1	tensin 1	2,64	7,47	27,85	1,17E-108	2,37E-105
205862_at	2	2p25.1	GREB1	growth regulation by estrogen in breast cancer 1	2,05	4,40	27,51	6,52E-107	1,27E-103
223552_at	7	7q31.3	LRRC4	leucine rich repeat containing 4	0,80	6,83	27,39	2,63E-106	4,96E-103
232750_at	2	2q35-q36	TNS1	Tensin 1	1,44	5,75	27,33	5,30E-106	9,66E-103
207437_at	14	14q	NOVA1	neuro-oncological ventral antigen 1	1,12	4,07	27,19	3,00E-105	5,29E-102
241505_at	NA	NA	---	---	2,21	7,66	27,07	1,20E-104	2,06E-101
227862_at	1	1p36.11	TRNP1	TMF1-regulated nuclear protein 1	2,05	6,66	26,98	3,63E-104	6,02E-101
238275_at	17	17q21.2-q21.3	HAP1	huntingtin-associated protein 1	1,01	5,92	26,67	1,48E-102	2,39E-99
229339_at	NA	NA	MYOCD	myocardin	1,48	5,86	26,63	2,32E-102	3,63E-99
223689_at	17	17q21.32	IGF2BP1	insulin-like growth factor 2 mRNA binding protein 1	0,60	5,98	26,54	6,82E-102	1,04E-98
235501_at	NA	NA	---	---	1,43	6,56	26,47	1,47E-101	2,17E-98
1553734_at	14	14q32.2	AK7	adenylate kinase 7	1,63	5,48	26,41	3,32E-101	4,77E-98
206460_at	1	1p36.32	AJAP1	adherens junctions associated protein 1	1,35	5,50	26,37	5,04E-101	7,06E-98
231455_at	2	2p25.2	FLJ42418	FLJ42418 protein	2,13	5,46	26,12	1,01E-99	1,38E-96
203324_s_at	7	7q31.1	CAV2	caveolin 2	1,60	4,77	25,60	5,39E-97	7,18E-94
241239_at	17	17p11.2	---	---	0,94	5,54	25,59	5,98E-97	7,78E-94
214110_s_at	2	2p11.1	---	---	1,35	6,54	25,58	6,25E-97	7,95E-94
205794_s_at	14	14q	NOVA1	neuro-oncological ventral antigen 1	1,10	5,26	25,48	2,10E-96	2,60E-93
1564149_at	NA	NA	---	---	1,53	6,35	25,30	1,96E-95	2,38E-92
204160_s_at	6	6p12.3	ENPP4	ectonucleotide pyrophosphatase/phosphodiesterase 4 (putative)	1,80	5,86	25,21	5,41E-95	6,43E-92
215790_at	1	1p36.32	AJAP1	adherens junctions associated protein 1	0,94	5,13	25,16	1,02E-94	1,18E-91
1563182_at	2	2q24.1	ACVR1C	activin A receptor, type IC	1,51	5,02	25,15	1,07E-94	1,21E-91
239246_at	13	13q32.2	FARP1	FERM, RhoGEF (ARHGEF) and pleckstrin domain protein 1 (chonc	1,66	5,58	25,12	1,53E-94	1,71E-91
235694_at	20	20q13.3-qter	TCFL5	transcription factor-like 5 (basic helix-loop-helix)	2,42	7,44	24,95	1,23E-93	1,35E-90
222943_at	4	4p15.31	GBA3	glucosidase, beta, acid 3 (cytosolic)	1,90	5,73	24,92	1,79E-93	1,92E-90
203184_at	5	5q23-q31	FBN2	fibrillin 2	1,91	5,49	24,88	2,80E-93	2,94E-90
202382_s_at	5	5q21	GNPDA1	glucosamine-6-phosphate deaminase 1	1,01	6,06	24,87	3,13E-93	3,23E-90
202517_at	4	4p16.1-p15	CRMP1	collapsin response mediator protein 1	1,97	8,19	24,74	1,49E-92	1,51E-89
238617_at	NA	NA	---	---	1,19	5,84	24,43	6,29E-91	6,25E-88
1569348_at	22	22q11.2	psiTPTE22	TPTE pseudogene	1,62	5,36	24,40	9,29E-91	9,07E-88
210058_at	6	6p21.31	MAPK13	mitogen-activated protein kinase 13	0,86	6,33	24,24	5,93E-90	5,68E-87
201976_s_at	5	5p15.1-p14.3	MYO10	myosin X	2,35	6,66	24,15	1,73E-89	1,63E-86
229230_at	3	3q29	OSTalpha	organic solute transporter alpha	1,52	5,36	24,07	4,90E-89	4,54E-86
223468_s_at	15	15q26.1	RGMA	RGM domain family, member A	1,74	7,45	24,06	5,50E-89	5,02E-86
211222_s_at	17	17q21.2-q21.3	HAP1	huntingtin-associated protein 1	0,78	6,82	23,97	1,66E-88	1,49E-85
224725_at	18	18q11.2	MIB1	mindbomb homolog 1 (Drosophila)	1,92	7,28	23,90	3,81E-88	3,36E-85
229638_at	16	16q12.2	IRX3	iroquois homeobox 3	2,57	5,57	23,88	4,70E-88	4,08E-85
213558_at	7	7q11.23-q21.3	PCLO	piccolo (presynaptic cytomatrix protein)	2,49	6,23	23,86	5,85E-88	4,99E-85
219954_s_at	4	4p15.31	GBA3	glucosidase, beta, acid 3 (cytosolic)	1,47	5,90	23,78	1,47E-87	1,23E-84
218804_at	11	11q13.3	ANO1	anoctamin 1, calcium activated chloride channel	2,10	5,23	23,73	2,90E-87	2,40E-84
213122_at	8	8q22.1	TSPYL5	TSPYL-like 5	2,61	6,28	23,53	3,11E-86	2,54E-83
244218_at	NA	NA	---	---	0,78	5,71	23,51	3,99E-86	3,21E-83
201911_s_at	13	13q32.2	FARP1	FERM, RhoGEF (ARHGEF) and pleckstrin domain protein 1 (chonc	1,35	6,34	23,49	5,25E-86	4,16E-83
204914_s_at	2	2p25	SOX11	SRY (sex determining region Y)-box 11	3,84	7,10	23,44	8,88E-86	6,94E-83
217628_at	6	6p21.1-p12.1	CLIC5	chloride intracellular channel 5	0,87	5,99	23,30	4,77E-85	3,67E-82
204161_s_at	6	6p12.3	ENPP4	ectonucleotide pyrophosphatase/phosphodiesterase 4 (putative)	1,22	5,02	23,16	2,75E-84	2,09E-81
242133_s_at	NA	NA	---	---	0,93	6,06	23,09	6,04E-84	4,53E-81
226548_at	16	16p11.2	SBK1	SH3-binding domain kinase 1	1,14	7,27	23,09	6,22E-84	4,59E-81
230923_at	3	3p14.1	FAM19A1	family with sequence similarity 19 (chemokine (C-C motif)-like),	1,74	5,45	22,93	3,95E-84	2,88E-80
211891_s_at	2	2q22	ARHGEF4	Rho guanine nucleotide exchange factor (GEF) 4	0,70	6,14	22,92	4,49E-83	3,23E-80
204751_x_at	18	18q12.1	DSC2	desmocollin 2	0,92	4,60	22,89	6,87E-83	4,88E-80
218625_at	6	6p25.1	NRN1	neuritin 1	3,49	7,84	22,80	1,88E-82	1,31E-79
228158_at	1	1q21.1	LOC645166 ///	lymphocyte-specific protein 1 pseudogene /// lymphocyte-specif	1,23	6,56	22,78	2,66E-82	1,84E-79
238133_at	NA	NA	---	---	1,30	6,25	22,42	1,96E-80	1,34E-77
210650_s_at	7	7q11.23-q21.3	PCLO	piccolo (presynaptic cytomatrix protein)	2,31	5,46	22,41	2,12E-80	1,43E-77
204849_at	20	20q13.3-qter	TCFL5	transcription factor-like 5 (basic helix-loop-helix)	2,50	9,19	22,41	2,17E-80	1,44E-77
215149_at	NA	NA	---	---	1,07	5,88	22,37	3,37E-80	2,22E-77
204913_s_at	2	2p25	SOX11	SRY (sex determining region Y)-box 11	3,59	6,41	22,35	4,37E-80	2,84E-77
218078_s_at	3	3p21.31	ZDHC3	zinc finger, DHHC-type containing 3	0,81	7,59	22,27	1,11E-79	7,14E-77
227996_at	13	13q32.2	FARP1	FERM, RhoGEF (ARHGEF) and pleckstrin domain protein 1 (chonc	0,64	5,57	22,24	1,54E-79	9,76E-77

242881_x_at	NA	NA	---	---	2,80	5,23	22,17	3,86E-79	2,43E-76
205952_at	2	2p23	KCNK3	potassium channel, subfamily K, member 3	2,05	5,72	22,15	4,72E-79	2,93E-76
208056_s_at	16	16q24	CBFA2T3	core-binding factor, runt domain, alpha subunit 2; translocated t	1,53	8,57	22,15	4,83E-79	2,97E-76
235492_at	6	6q22.31	RNF217	ring finger protein 217	0,83	5,11	22,06	1,35E-78	8,18E-76
240950_s_at	19	19q13.33	CCDC155	coiled-coil domain containing 155	1,40	6,04	21,96	4,64E-78	2,79E-75
203463_s_at	17	17p11.2	EPN2	epsin 2	0,38	6,38	21,83	2,19E-77	1,30E-74
218077_s_at	3	3p21.31	ZDHC3	zinc finger, DHHC-type containing 3	0,65	6,77	21,73	7,07E-77	4,16E-74
215717_s_at	5	5q23-q31	FBN2	fibrillin 2	1,10	4,54	21,71	9,67E-77	5,62E-74
1562713_a_at	18	18q22-q23	NETO1	neuropilin (NRP) and tolloid (TLL)-like 1	1,50	6,24	21,68	1,36E-76	7,85E-74
204915_s_at	2	2p25	SOX11	SRY (sex determining region Y)-box 11	2,59	6,54	21,63	2,29E-76	1,30E-73
236236_at	NA	NA	WNK3	WNK lysine deficient protein kinase 3	0,54	5,15	21,48	1,49E-75	8,39E-73
1552736_a_at	18	18q22-q23	NETO1	neuropilin (NRP) and tolloid (TLL)-like 1	1,65	5,86	21,46	1,86E-75	1,04E-72
218813_s_at	9	9q34	SH3GLB2	SH3-domain GRB2-like endophilin B2	1,51	7,24	21,37	5,15E-75	2,84E-72
210059_s_at	6	6p21.31	MAPK13	mitogen-activated protein kinase 13	0,64	6,11	21,29	1,42E-74	7,74E-72
208690_s_at	10	10q22-q26.3	PDLIM1	PDZ and LIM domain 1	-1,92	11,14	-21,28	1,61E-74	8,74E-72
201910_at	13	13q32.2	FARP1	FERM, RhoGEF (ARHGEF) and pleckstrin domain protein 1 (chonc	0,93	6,72	21,16	6,21E-74	3,33E-71
239942_at	NA	NA	---	---	1,83	5,44	21,00	4,22E-73	2,24E-70
239118_at	1	1p13	KCNA2	potassium voltage-gated channel, shaker-related subfamily, mer	0,96	5,38	20,97	6,62E-73	3,48E-70
203038_at	6	6q22.2-q22.3	PTPRK	protein tyrosine phosphatase, receptor type, K	2,67	6,20	20,94	9,25E-73	4,82E-70
244107_at	NA	NA	---	---	1,13	4,90	20,90	1,45E-72	7,48E-70
224726_at	18	18q11.2	MIB1	mindbomb homolog 1 (Drosophila)	1,65	7,29	20,89	1,56E-72	7,99E-70
204750_s_at	18	18q12.1	DSC2	desmocollin 2	0,55	5,03	20,86	2,46E-72	1,25E-69
231015_at	3	3q13-q21	KLF15	Kruppel-like factor 15	0,51	6,26	20,85	2,50E-72	1,25E-69
224720_at	18	18q11.2	MIB1	mindbomb homolog 1 (Drosophila)	2,02	7,68	20,84	2,97E-72	1,48E-69
1555168_a_at	7	7q11	CALN1	calneuron 1	1,22	6,46	20,77	6,50E-72	3,20E-69
243159_x_at	NA	NA	---	---	1,79	4,77	20,73	1,14E-71	5,59E-69
202789_at	20	20q12-q13.1	PLCG1	phospholipase C, gamma 1	0,74	7,39	20,71	1,40E-71	6,75E-69
224907_s_at	9	9q34	SH3GLB2	SH3-domain GRB2-like endophilin B2	0,98	7,25	20,69	1,68E-71	8,04E-69
242563_at	NA	NA	---	---	1,41	6,57	20,67	2,30E-71	1,09E-68
239673_at	NA	NA	---	---	2,34	6,88	20,64	3,32E-71	1,56E-68
209227_at	8	8p22	TUSC3	tumor suppressor candidate 3	0,69	4,73	20,61	4,72E-71	2,21E-68
215789_s_at	1	1p36.32	AJAP1	adherens junctions associated protein 1	0,73	6,12	20,52	1,27E-70	5,86E-68
203910_at	1	1p22.1	ARHGAP29	Rho GTPase activating protein 29	2,62	7,03	20,42	4,30E-70	1,97E-67
226473_at	17	17q25.3	CBX2	chromobox homolog 2	0,89	7,04	20,41	4,92E-70	2,24E-67
223885_at	7	7q11	CALN1	calneuron 1	1,90	6,64	20,20	5,55E-69	2,51E-66
221246_x_at	2	2q35-q36	TNS1	tensin 1	0,60	6,63	20,17	8,88E-69	3,98E-66
235500_at	14	14q11.2	HNRNPC	heterogeneous nuclear ribonucleoprotein C (C1/C2)	1,02	6,95	20,14	1,18E-68	5,25E-66
213017_at	18	18q11.2	ABHD3	abhydrolase domain containing 3	1,65	8,61	20,12	1,50E-68	6,61E-66
237398_at	NA	NA	---	---	0,85	6,22	20,07	2,63E-68	1,15E-65
1559910_at	NA	NA	---	---	1,71	6,39	20,05	3,27E-68	1,42E-65
230698_at	7	7q11	CALN1	calneuron 1	2,30	5,84	20,05	3,54E-68	1,52E-65
1554140_at	1	1p31.3	WDR78	WD repeat domain 78	1,62	5,35	20,00	6,53E-68	2,79E-65
233850_s_at	20	20p13	EBF4	early B-cell factor 4	0,57	6,89	19,98	7,97E-68	3,38E-65
233609_at	6	6q22.2-q22.3	PTPRK	Protein tyrosine phosphatase, receptor type, K	1,67	5,02	19,94	1,32E-67	5,56E-65
215006_at	NA	NA	---	---	1,47	9,49	19,89	2,20E-67	9,18E-65
236430_at	16	16q22.1	TMED6	transmembrane emp24 protein transport domain containing 6	2,63	7,91	19,82	4,96E-67	2,06E-64
1557103_a_at	19	19q13.32	LMTK3	lemur tyrosine kinase 3	0,65	5,12	19,81	5,93E-67	2,44E-64
204743_at	3	3q13.2	TAGLN3	transgelin 3	0,55	6,35	19,79	7,52E-67	3,07E-64
220276_at	12	12p12.3	RERGL	RERGL/RAS-like	1,30	5,05	19,78	7,97E-67	3,23E-64
244350_at	5	5p15.1-p14.3	MYO10	myosin X	0,68	4,61	19,77	9,71E-67	3,90E-64
203925_at	1	1p22.1	GCLM	glutamate-cysteine ligase, modifier subunit	1,29	6,86	19,76	1,02E-66	4,06E-64
203431_s_at	11	11q24-q25	ARHGAP32	Rho GTPase activating protein 32	1,17	5,95	19,74	1,38E-66	5,46E-64
227634_at	10	10q26.3	STK32C	serine/threonine kinase 32C	0,65	6,70	19,65	4,09E-66	1,61E-63
219360_s_at	19	19q13.33	TRPM4	transient receptor potential cation channel, subfamily M, memb	2,08	6,50	19,61	6,10E-66	2,38E-63
232549_at	21	21q11	RBM11	RNA binding motif protein 11	1,01	4,58	19,59	7,65E-66	2,97E-63
220002_at	1	1q44	KIF26B	kinesin family member 26B	0,50	5,49	19,59	7,81E-66	3,01E-63
218608_at	1	1p36	ATP13A2	ATPase type 13A2	-0,73	6,92	-19,54	1,40E-65	5,35E-63
226549_at	16	16p11.2	SBK1	SH3-binding domain kinase 1	0,59	6,56	19,49	2,47E-65	9,36E-63
211548_s_at	4	4q34-q35	HPGD	hydroxyprostaglandin dehydrogenase 15-(NAD)	0,94	4,92	19,33	1,65E-64	6,22E-62
201334_s_at	11	11q23.3	ARHGEF12	Rho guanine nucleotide exchange factor (GEF) 12	1,75	7,50	19,29	2,73E-64	1,02E-61
212158_at	8	8q22-q23	SDC2	syndecan 2	2,42	7,42	19,26	3,94E-64	1,47E-61
203914_x_at	4	4q34-q35	HPGD	hydroxyprostaglandin dehydrogenase 15-(NAD)	0,93	5,14	19,25	4,17E-64	1,54E-61
226885_at	NA	NA	---	---	0,96	4,94	19,21	6,56E-64	2,41E-61
1554026_a_at	5	5p15.1-p14.3	MYO10	myosin X	2,88	8,04	19,19	8,75E-64	3,19E-61
242196_at	NA	NA	ARHGAP32	Rho GTPase activating protein 32	0,90	4,96	19,19	8,93E-64	3,23E-61
229912_at	7	7p22.2	SDK1	sidekick homolog 1, cell adhesion molecule (chicken)	0,85	5,49	19,18	9,69E-64	3,49E-61
211795_s_at	5	5p13.1	FYB	FYN binding protein	1,75	6,74	19,18	9,83E-64	3,51E-61
232282_at	X	Xp11.23-p11.21	WNK3	WNK lysine deficient protein kinase 3	0,63	4,99	19,16	1,25E-63	4,42E-61
243742_at	NA	NA	LOC100505797	hypothetical LOC100505797	1,15	5,46	19,13	1,80E-63	6,36E-61
212399_s_at	3	3p25.2	VGLL4	vestigial like 4 (Drosophila)	0,92	8,45	19,04	5,19E-63	1,82E-60
220227_at	20	20q13.3	CDH4	cadherin 4, type 1, R-cadherin (retinal)	1,26	6,26	19,03	5,87E-63	2,04E-60
226171_at	3	3p21.31	ZDHC3	zinc finger, DHHC-type containing 3	0,56	6,57	19,00	8,13E-63	2,81E-60
212063_at	11	11p13	CD44	CD44 molecule (Indian blood group)	-1,82	9,65	-18,98	9,95E-63	3,42E-60
227266_s_at	5	5p13.1	FYB	FYN binding protein	1,95	6,94	18,91	2,19E-62	7,47E-60
203913_s_at	4	4q34-q35	HPGD	hydroxyprostaglandin dehydrogenase 15-(NAD)	1,61	4,86	18,91	2,27E-62	7,70E-60
220692_at	7	7q22.1	---	---	0,78	7,23	18,91	2,39E-62	8,06E-60
243952_at	22	22q11.2	---	---	0,81	5,55	18,90	2,59E-62	8,68E-60
206866_at	20	20q13.3	CDH4	cadherin 4, type 1, R-cadherin (retinal)	1,11	6,56	18,89	2,79E-62	9,32E-60
219471_at	13	13q14.12	C13orf18	chromosome 13 open reading frame 18	1,74	8,62	18,85	4,55E-62	1,51E-59
235801_at	NA	NA	TUSC3	tumor suppressor candidate 3	0,60	4,22	18,82	6,52E-62	2,15E-59
233518_at	NA	NA	---	---	0,73	4,99	18,78	9,93E-62	3,25E-59
221042_s_at	14	14q32.13	CLMN	calmin (calponin-like, transmembrane)	0,85	6,19	18,69	3,00E-61	9,76E-59
215516_at	7	7q22-q31.2	LAMB4	laminin, beta 4	0,78	4,37	18,65	4,58E-61	1,48E-58
212154_at	8	8q22-q23	SDC2	syndecan 2	2,02	7,45	18,64	5,57E-61	1,79E-58
219093_at	2	2q36.3	PID1	phosphotyrosine interaction domain containing 1	1,04	5,04	18,62	6,93E-61	2,21E-58
232235_at	18	18q22.1	DSEL	dermatan sulfate epimerase-like	1,29	4,60	18,59	9,61E-61	3,05E-58
209695_at	8	8q24.3	PTP4A3	protein tyrosine phosphatase type IVA, member 3	1,69	8,56	18,58	1,03E-60	3,27E-58
215843_s_at	10	10q23-q24	TLL2	tolloid-like 2	0,52	5,84	18,51	2,38E-60	7,49E-58
204115_at	7	7q21	GNG11	guanine nucleotide binding protein (G protein), gamma 11	3,03	8,88	18,48	3,34E-60	1,04E-57

202668_at	13	13q33	EFNB2	ephrin-B2	1,85	7,44	14,40	2,24E-40	2,77E-38
1555492_a_at	12	12q14.2-q15	BEST3	bestrophin 3	0,63	4,83	14,40	2,27E-40	2,79E-38
212443_at	3	3p21.31	NBEAL2	neurobeachin-like 2	-0,69	7,74	-14,39	2,51E-40	3,09E-38
205123_s_at	9	9q31	TMEFF1	transmembrane protein with EGF-like and two follistatin-like dor	0,64	4,47	14,37	3,02E-40	3,70E-38
204591_at	3	3p26.1	CHL1	cell adhesion molecule with homology to L1CAM (close homolog	0,64	4,47	14,37	3,17E-40	3,87E-38
203860_at	13	13q32	PCCA	propionyl CoA carboxylase, alpha polypeptide	1,43	6,43	14,36	3,59E-40	4,38E-38
212956_at	4	4q31.21	TBC1D9	TBC1 domain family, member 9 (with GRAM domain)	1,81	7,02	14,35	4,00E-40	4,87E-38
220230_s_at	11	11p15.4	CYB5R2	cytochrome b5 reductase 2	1,58	7,33	14,34	4,21E-40	5,11E-38
236718_at	5	5p15.1-p14.3	MYO10	myosin X	0,47	4,64	14,31	6,24E-40	7,57E-38
226216_at	19	19p13.3-p13.2	INSR	insulin receptor	0,83	7,28	14,30	6,34E-40	7,67E-38
206274_s_at	1	1pter-p36.11	CROCC	ciliary rootlet coiled-coil, rootletin	-0,27	6,29	-14,30	6,79E-40	8,20E-38
243461_at	NA	NA	---	---	0,65	5,16	14,29	7,61E-40	9,16E-38
228340_at	15	15q22	TLE3	transducin-like enhancer of split 3 (E(sp1) homolog, Drosophila)	0,84	7,02	14,26	1,04E-39	1,25E-37
226035_at	16	16p12.1	USP31	ubiquitin specific peptidase 31	0,81	6,25	14,24	1,20E-39	1,44E-37
1556354_s_at	19	19p13.2	RGL3	ral guanine nucleotide dissociation stimulator-like 3	0,29	4,48	14,23	1,35E-39	1,61E-37
233072_at	9	9q34	NTNG2	netrin G2	0,73	6,75	14,23	1,40E-39	1,67E-37
232914_s_at	11	11q14	SYTL2	synaptotagmin-like 2	1,36	6,59	14,23	1,48E-39	1,76E-37
226764_at	4	4q31.22	ZNF827	zinc finger protein 827	0,84	6,21	14,21	1,65E-39	1,96E-37
203365_s_at	16	16q13-q21	MMP15	matrix metalloproteinase 15 (membrane-inserted)	0,39	6,57	14,17	2,63E-39	3,12E-37
214369_s_at	11	11q13	RASGRP2	RAS guanyl releasing protein 2 (calcium and DAG-regulated)	-0,76	9,59	-14,16	2,87E-39	3,39E-37
230670_at	3	3q25.1	IGSF10	immunoglobulin superfamily, member 10	0,66	6,26	14,16	2,92E-39	3,45E-37
209921_at	4	4q28-q32	SLC7A11	solute carrier family 7, (cationic amino acid transporter, y+ syste	0,60	5,32	14,15	3,28E-39	3,86E-37
203895_at	20	20p12	PLCB4	phospholipase C, beta 4	1,22	4,82	14,15	3,34E-39	3,93E-37
241506_at	NA	NA	---	---	0,59	4,33	14,13	3,90E-39	4,58E-37
202087_s_at	9	9q21-q22	CTSL1	cathepsin L1	0,41	6,72	14,12	4,44E-39	5,19E-37
229459_at	22	22q13.32	FAM19A5	family with sequence similarity 19 (chemokine (C-C motif)-like),	1,93	5,36	14,12	4,57E-39	5,34E-37
1553102_a_at	5	5q33.1	CCDC69	coiled-coil domain containing 69	-1,06	7,72	-14,09	5,84E-39	6,81E-37
1558815_at	4	4q35.1	SORBS2	sorbin and SH3 domain containing 2	0,47	4,49	14,09	6,36E-39	7,40E-37
223539_s_at	5	5q12.2-q13.3	SERF1A /// SEF	small EDRK-rich factor 1A (telomeric) /// small EDRK-rich factor 1	0,45	7,40	14,08	6,51E-39	7,55E-37
202598_at	1	1q21	S100A13	S100 calcium binding protein A13	-0,94	8,90	-14,08	6,90E-39	7,99E-37
202825_at	4	4q35	SLC25A4	solute carrier family 25 (mitochondrial carrier; adenine nucleotic	0,42	7,10	14,08	7,02E-39	8,11E-37
235121_at	19	19q13.43	ZNF542	zinc finger protein 542	0,66	6,01	14,07	7,63E-39	8,80E-37
204288_s_at	4	4q35.1	SORBS2	sorbin and SH3 domain containing 2	0,55	5,90	14,06	8,48E-39	9,76E-37
1554451_s_at	12	12q13.2	DNAJC14	DnaJ (Hsp40) homolog, subfamily C, member 14	0,54	6,58	14,06	8,66E-39	9,95E-37
216696_s_at	19	19q13.1	PRODH2	proline dehydrogenase (oxidase) 2	0,58	6,62	14,05	9,19E-39	1,05E-36
240532_at	20	20q11.23	SLC32A1	solute carrier family 32 (GABA vesicular transporter), member 1	1,08	6,09	14,05	9,65E-39	1,10E-36
231859_at	14	14q32.2	C14orf132	chromosome 14 open reading frame 132	0,48	6,37	14,05	9,78E-39	1,12E-36
203523_at	11	11p15.5	LSP1	lymphocyte-specific protein 1	-1,22	7,84	-14,03	1,12E-38	1,28E-36
212960_at	4	4q31.21	TBC1D9	TBC1 domain family, member 9 (with GRAM domain)	0,56	6,40	14,03	1,16E-38	1,32E-36
204906_at	6	6q27	RPS6KA2	ribosomal protein S6 kinase, 90kDa, polypeptide 2	0,37	7,01	14,03	1,19E-38	1,35E-36
212886_at	5	5q33.1	CCDC69	coiled-coil domain containing 69	-1,01	7,91	-14,03	1,19E-38	1,35E-36
228570_at	12	12q23.3	BTBD11	BTB (POZ) domain containing 11	-1,22	7,05	-14,02	1,24E-38	1,40E-36
240572_s_at	12	12p13.31	LOC374443	CLR pseudogene	-1,07	8,19	-14,00	1,64E-38	1,85E-36
241917_at	NA	NA	---	---	0,91	5,61	13,99	1,80E-38	2,03E-36
244428_at	2	2p23	DNMT3A	DNA (cytosine-5-)-methyltransferase 3 alpha	0,58	7,07	13,99	1,84E-38	2,06E-36
214969_at	14	14q24.3-q31	MAP3K9	mitogen-activated protein kinase kinase kinase 9	0,32	6,09	13,97	2,06E-38	2,31E-36
223196_s_at	1	1p35.3	SESN2	sestrin 2	0,97	7,78	13,96	2,49E-38	2,78E-36
1553998_at	X	Xq13.1	DMRTC1 /// DM	DMRT-like family C1 /// DMRT-like family C1B	0,44	5,45	13,95	2,62E-38	2,93E-36
226698_at	5	5q31.3	FCHSD1	FCH and double SH3 domains 1	0,55	6,24	13,94	2,89E-38	3,22E-36
1559420_x_at	10	10p12	CACNB2	calcium channel, voltage-dependent, beta 2 subunit	0,85	5,08	13,94	2,93E-38	3,25E-36
205005_s_at	10	10p13	NMT2	N-myristoyltransferase 2	0,94	7,04	13,94	3,06E-38	3,40E-36
208405_s_at	6	6q21	CD164	CD164 molecule, sialomucin	-0,79	10,63	-13,92	3,55E-38	3,92E-36
227647_at	11	11q13-q14	KCNE3	potassium voltage-gated channel, Isk-related family, member 3	1,19	6,91	13,92	3,72E-38	4,11E-36
214743_at	7	7q22.1	CUX1	cut-like homeobox 1	0,73	9,98	13,91	4,10E-38	4,52E-36
218557_at	3	3q12.2	NIT2	nitrilase family, member 2	-0,73	7,50	-13,90	4,28E-38	4,71E-36
206011_at	11	11q23	CASP1	caspase 1, apoptosis-related cysteine peptidase (interleukin 1, br	-1,05	5,79	-13,90	4,50E-38	4,94E-36
215087_at	15	15q24.2	C15orf39	chromosome 15 open reading frame 39	-1,02	7,01	-13,89	5,25E-38	5,75E-36
238889_at	2	2p23.3	AGBL5	ATP/GTP binding protein-like 5	0,26	5,08	13,87	5,87E-38	6,42E-36

Supplementary Table 2. Differentially regulated genes in ETV6-RUNX1 positive CB-CD34+ cells (40 hours after transduction)

Probeset	p-value	Name	LogFI	FI
44783_s_at	0,02	HEY1	3,22	24,92
218839_at	0,00	HEY1	2,78	16,10
204537_s_at	0,01	GABRE	2,46	11,74
207741_x_at	0,04	TPSAB1	2,31	10,04
207808_s_at	0,03	PROS1	2,27	9,64
223658_at	0,04	KCNK6	2,24	9,42
210805_x_at	0,01	RUNX1	2,24	9,36
216474_x_at	0,04	TPSB2	2,19	8,96
203661_s_at	0,02	TMOD1	2,18	8,81
204416_x_at	0,04	APOC1	2,15	8,62
207134_x_at	0,04	TPSB2	2,09	8,08
207526_s_at	0,02	IL1RL1	2,08	8,02
213515_x_at	0,04	HBG1	2,06	7,86
212472_at	0,01	MICAL2	1,96	7,12
212771_at	0,01	FAM171A1	1,96	7,08
205683_x_at	0,04	TPSAB1	1,95	7,04
205389_s_at	0,01	ANK1	1,90	6,69
1552378_s_at	0,01	RDH10	1,87	6,52
210139_s_at	0,00	PMP22	1,80	6,04
226021_at	0,01	RDH10	1,78	5,95
215382_x_at	0,02	TPSAB1	1,76	5,80
202479_s_at	0,03	TRIB2	1,74	5,72
201334_s_at	0,03	ARHGEF12	1,68	5,38
227703_s_at	0,03	SYTL4	1,67	5,32
201694_s_at	0,02	EGR1	1,64	5,14
218729_at	0,04	LXN	1,63	5,08
227404_s_at	0,00	EGR1	1,62	5,04
227461_at	0,02	STON2	1,61	5,02
210504_at	0,04	KLF1	1,61	5,02
207067_s_at	0,02	HDC	1,56	4,77
202284_s_at	0,04	CDKN1A	1,56	4,74
1553328_a_at	0,02	SLC18A2	1,56	4,74
202949_s_at	0,04	FHL2	1,55	4,69
210360_s_at	0,03	MTSS1	1,54	4,67
203561_at	0,02	FCGR2A	1,54	4,66
216191_s_at	0,03	NA	1,54	4,65
211734_s_at	0,01	FCER1A	1,53	4,60
226751_at	0,02	CNRIP1	1,50	4,47
210762_s_at	0,04	DLC1	1,50	4,46
202859_x_at	0,05	IL8	1,48	4,37
202481_at	0,04	DHRS3	1,38	3,98
212089_at	0,01	LMNA	1,37	3,94
201333_s_at	0,05	ARHGEF12	1,36	3,89

201147_s_at	0,04	TIMP3	1,35	3,84
224822_at	0,04	DLC1	1,34	3,83
1555590_a_at	0,05	GATA1	1,33	3,78
226794_at	0,02	STXBP5	1,32	3,76
234541_s_at	0,03	ARHGEF12	1,32	3,74
241615_x_at	0,04	NA	1,29	3,63
211743_s_at	0,04	PRG2	1,22	3,40
211005_at	0,01	LAT	1,22	3,38
206726_at	0,03	HPGDS	1,21	3,36
201150_s_at	0,04	TIMP3	1,21	3,34
1555950_a_at	0,04	CD55	1,20	3,31
209723_at	0,02	SERPINB9	1,18	3,27
204187_at	0,02	GMPR	1,13	3,11
201170_s_at	0,00	BHLHE40	1,12	3,07
211965_at	0,02	ZFP36L1	1,11	3,04
230416_at	0,01	NA	1,10	2,99
227155_at	0,00	LMO4	1,08	2,95
205159_at	0,01	CSF2RB	1,08	2,93
201926_s_at	0,02	CD55	1,07	2,90
209870_s_at	0,02	APBA2	1,04	2,83
201925_s_at	0,00	CD55	1,04	2,82
204683_at	0,02	ICAM2	1,02	2,76
206493_at	0,03	ITGA2B	0,98	2,65
1561405_s_at	0,02	CATSPER2	0,96	2,62
224991_at	0,03	CMIP	0,96	2,61
210358_x_at	0,04	GATA2	0,96	2,61
223391_at	0,05	SGPP1	0,94	2,55
214899_at	0,04	ZNF780B	0,93	2,53
230391_at	0,04	CD84	0,93	2,53
224992_s_at	0,03	CMIP	0,91	2,49
226694_at	0,00	AKAP2	0,90	2,47
209205_s_at	0,00	LMO4	0,88	2,42
203196_at	0,01	ABCC4	0,84	2,32
212335_at	0,00	GNS	0,83	2,30
1563357_at	0,03	NA	0,83	2,30
53720_at	0,02	C19orf66	0,81	2,26
206675_s_at	0,02	SKIL	0,80	2,23
223666_at	0,04	SNX5	0,80	2,22
209710_at	0,02	GATA2	0,79	2,19
202974_at	0,02	MPP1	0,74	2,10
200648_s_at	0,01	GLUL	0,74	2,09
217202_s_at	0,00	GLUL	0,74	2,09
208093_s_at	0,02	NDEL1	0,73	2,07
226921_at	0,02	UBR1	0,72	2,05
229336_at	0,04	ST3GAL2	0,71	2,03
231925_at	0,04	NA	0,70	2,02
224414_s_at	0,04	CARD6	0,67	1,95

231643_s_at	0,04	CMIP	0,66	1,94
230795_at	0,02	NA	0,63	1,88
234985_at	0,03	LDLRAD3	0,62	1,86
226994_at	0,04	DNAJA2	0,60	1,81
204507_s_at	0,03	PPP3R1	0,59	1,81
225799_at	0,04	NA	0,59	1,80
227877_at	0,05	C5orf39	0,58	1,79
210557_x_at	0,01	CSF1	0,58	1,78
215111_s_at	0,04	TSC22D1	0,57	1,76
202377_at	0,04	LEPROT	0,55	1,74
221249_s_at	0,04	FAM117A	0,53	1,70
221778_at	0,04	JHDM1D	0,53	1,69
212919_at	0,05	DCP2	0,51	1,66
223106_at	0,03	TMEM14C	0,50	1,65
221269_s_at	0,02	SH3BGRL3	0,49	1,64
219132_at	0,01	PELI2	0,49	1,64
1556060_a_at	0,01	ZNF451	0,48	1,62
209536_s_at	0,01	EHD4	0,48	1,62
234976_x_at	0,02	NA	0,48	1,61
207157_s_at	0,03	GNG5	0,47	1,59
217416_x_at	0,01	NA	0,46	1,59
201010_s_at	0,02	TXNIP	0,46	1,59
1552980_at	0,03	HAS3	0,46	1,58
212258_s_at	0,02	SMARCA2	0,46	1,58
223335_at	0,04	TMEM69	0,46	1,58
212268_at	0,01	SERPIN1	0,45	1,57
225834_at	0,02	NA	0,44	1,56
223303_at	0,03	FERMT3	0,43	1,53
201720_s_at	0,04	LAPTM5	0,42	1,52
224565_at	0,03	NEAT1	0,42	1,52
33132_at	0,04	CPSF1	0,42	1,52
201844_s_at	0,03	RYBP	0,41	1,51
202599_s_at	0,03	NRIP1	-0,41	1,51
201513_at	0,02	TSN	-0,42	1,52
221707_s_at	0,04	VPS53	-0,42	1,53
218376_s_at	0,04	MICAL1	-0,44	1,55
222237_s_at	0,00	ZFP112	-0,44	1,56
225240_s_at	0,02	MSI2	-0,45	1,57
239314_at	0,02	NHLRC3	-0,45	1,57
224787_s_at	0,04	RAB18	-0,45	1,57
222045_s_at	0,04	PCIF1	-0,47	1,60
219789_at	0,02	NPR3	-0,47	1,60
205596_s_at	0,02	SMURF2	-0,47	1,60
212844_at	0,04	RRP1B	-0,48	1,61
204304_s_at	0,02	PROM1	-0,48	1,61
243002_at	0,00	NA	-0,48	1,61
210894_s_at	0,04	CEP250	-0,48	1,61

224467_s_at	0,01	PDCD2L	-0,49	1,63
237118_at	0,04	NA	-0,49	1,63
225150_s_at	0,03	RTKN	-0,52	1,68
223236_at	0,04	CCDC55	-0,52	1,69
202314_at	0,04	CYP51A1	-0,53	1,70
237518_at	0,03	NA	-0,54	1,71
236023_at	0,04	CDK9	-0,54	1,71
211791_s_at	0,04	KCNAB2	-0,54	1,72
240265_at	0,02	TRAF3IP3	-0,54	1,72
219109_at	0,01	SPAG16	-0,55	1,73
202247_s_at	0,00	MTA1	-0,55	1,74
204197_s_at	0,03	RUNX3	-0,55	1,74
205398_s_at	0,03	SMAD3	-0,55	1,74
229354_at	0,04	AHRR	-0,57	1,77
200974_at	0,04	ACTA2	-0,58	1,78
210570_x_at	0,01	MAPK9	-0,58	1,79
222845_x_at	0,04	TMBIM4	-0,58	1,79
209163_at	0,04	CYB561	-0,58	1,79
219420_s_at	0,04	C1orf163	-0,59	1,80
231982_at	0,04	C19orf77	-0,61	1,83
217611_at	0,01	ERICH1	-0,62	1,85
214452_at	0,05	BCAT1	-0,62	1,86
239016_at	0,01	NA	-0,62	1,86
219165_at	0,04	PDLIM2	-0,62	1,86
217853_at	0,02	TNS3	-0,62	1,87
214745_at	0,00	PLCH1	-0,64	1,89
238239_at	0,04	WDR27	-0,65	1,91
221542_s_at	0,03	ERLIN2	-0,65	1,91
225215_s_at	0,02	MTRF1L	-0,66	1,94
213094_at	0,03	GPR126	-0,67	1,95
208680_at	0,04	PRDX1	-0,68	1,97
215415_s_at	0,04	LYST	-0,70	2,01
204949_at	0,05	ICAM3	-0,70	2,02
229876_at	0,05	PHKA1	-0,71	2,03
209757_s_at	0,04	MYCN	-0,72	2,04
1565544_at	0,03	RNF141	-0,73	2,07
213937_s_at	0,04	FTSJ1	-0,75	2,11
205372_at	0,00	PLAG1	-0,75	2,12
215343_at	0,00	CCDC88C	-0,76	2,13
205213_at	0,04	ACAP1	-0,76	2,15
238670_at	0,02	RAD18	-0,77	2,16
229491_at	0,01	NHEDC2	-0,78	2,18
225828_at	0,04	DAGLB	-0,78	2,18
244000_at	0,03	NA	-0,81	2,25
1552562_at	0,04	ZNF570	-0,85	2,33
235887_at	0,04	NA	-0,86	2,35
226034_at	0,00	DUSP4	-0,87	2,40

231310_at	0,00	NA	-0,88	2,42
219207_at	0,03	EDC3	-0,93	2,53
231887_s_at	0,03	KIAA1274	-1,02	2,77
205196_s_at	0,02	AP1S1	-1,05	2,85
212489_at	0,01	COL5A1	-1,15	3,17
231775_at	0,04	TNFRSF10A	-1,23	3,41
1555320_a_at	0,03	STAB1	-1,23	3,42
1555339_at	0,02	RAP1A	-1,34	3,83
1568997_at	0,04	POLR1E	-1,40	4,07
1555340_x_at	0,00	RAP1A	-1,48	4,39
206310_at	0,03	SPINK2	-1,51	4,53
211597_s_at	0,05	HOPX	-2,00	7,37